

OPEN ACCESS

EDITED BY
Manoj Kumar Tembhre,
All India Institute of Medical Sciences, India

REVIEWED BY
Eva Reali,
University of Ferrar, Italy
Kunju Zhu,
University of Pittsburgh, United States
Ilan Bank,
Sheba Medical Center, Israel

*CORRESPONDENCE Stana Tokić ヌtokic@mefos.hr

RECEIVED 21 July 2025
ACCEPTED 25 September 2025
PUBLISHED 17 October 2025

CITATION

Jirouš Drulak M, Mihalj M, Štefanić M, Plužarić V, Šola M, Tolušić-Levak M, Marković M, Balogh P and Tokić S (2025) Psoriasis vulgaris leaves a dynamic imprint on circulating and skin γδ TCR repertoires shaped by disease severity, age, and sex. Front. Immunol. 16:1670364. doi: 10.3389/fimmu.2025.1670364

COPYRIGHT

© 2025 Jirouš Drulak, Mihalj, Štefanić, Plužarić, Šola, Tolušić-Levak, Marković, Balogh and Tokić. This is an open-access article distributed under the terms of the Creative Commons Attribution License (CC BY). The use, distribution or reproduction in other forums is permitted, provided the original author(s) and the copyright owner(s) are credited and that the original publication in this journal is cited, in accordance with accepted academic practice. No use, distribution or reproduction is permitted which does not comply with these terms.

Psoriasis vulgaris leaves a dynamic imprint on circulating and skin $\gamma\delta$ TCR repertoires shaped by disease severity, age, and sex

Maja Jirouš Drulak¹, Martina Mihalj^{2,3}, Mario Štefanić⁴, Vera Plužarić^{3,5}, Marija Šola³, Maja Tolušić-Levak^{3,6}, Marina Marković⁵, Peter Balogh⁷ and Stana Tokić^{5*}

¹Department of Medical Chemistry, Biochemistry and Clinical Chemistry, Faculty of Medicine, Josip Juraj Strossmayer University of Osijek, Osijek, Croatia, ²Department of Physiology and Immunology, Faculty of Medicine, Josip Juraj Strossmayer University of Osijek, Osijek, Croatia, ³Department of Dermatology and Venerology, University Hospital Osijek, Osijek, Croatia, ⁴Department of Nuclear Medicine and Oncology, Faculty of Medicine, Josip Juraj Strossmayer University of Osijek, Osijek, Croatia, ⁵Department of Laboratory Medicine and Pharmacy, Faculty of Medicine, Josip Juraj Strossmayer University of Osijek, Croatia, ⁶Department of Histology and Embryology, Faculty of Medicine, Josip Juraj Strossmayer University of Osijek, Croatia, ⁷Department of Immunology and Biotechnology, Faculty of Medicine, University of Pecs, Pecs, Hungary

Psoriasis vulgaris (PV) is a common, T cell mediated dermatosis with substantial systemic footprint. While $\alpha\beta$ T cells are well established drivers of PV, the role of $\gamma\delta$ T cells, including their abundance, clonal architecture and transcriptional programs in PV remain incompletely understood. To address this, we performed an integrated analysis of circulating and cutaneous $\gamma\delta$ cells from 65 patients with PV and 35 healthy controls using TCR repertoire sequencing, bulk transcriptomics, and flow cytometry. In PV, disease severity and age drove contraction of peripheral $\gamma\delta$ T cell repertoires, marked by loss of rare clonotypes and hyperexpansion patterns. Subset composition, segment usage, and CDR3 length of both skin and blood clonotypes were further modulated by age, disease severity, and sex, highlighting nuanced repertoire remodeling. TCRy clonotypes showed partial overlap between blood and skin, whereas TCR δ clonotypes remained private and tissue-specific, with no PV-specific clonotypes identified. Transcriptomic profiling indicated that circulating $\gamma\delta$ T cells adopt an activated, cytotoxic, tissue-homing phenotype, consistent with enhanced potential to migrate into and act within lesional skin, especially in a subset of patients. Collectively, these findings demonstrate that PV drives dynamic, clinically modulated remodeling of $\gamma\delta$ T cells across compartments, positioning them as dynamic elements of the psoriatic immune landscape and potential targets for future functional and therapeutic investigation.

KEYWORDS

Psoriasis vulgaris, $\gamma\delta$ T cells, TCR repertoire, transcriptome, RNA-Seq, skinimmunity

1 Introduction

Psoriasis vulgaris is a chronic erythematosquamous dermatosis of unknown etiology that usually persists for life. The characteristic features of the disease include skin plaques that are often accompanied by rheumatic, intestinal or cardiovascular manifestations of the disease. Both cutaneous and systemic disease features can be ameliorated by immunosuppressive (cyclosporine A, methotrexate) or cytokine-blocking, biologic therapy (anti-TNFα, anti-IL-23p19, anti-IL23p40, anti-IL-17A, and anti-IL-17) (1), alleviating symptoms in most but not all treated patients. Persistent PV has mostly been attributed to IFN-γ and IL-17A-producing αβT cell infiltrate (2–5), but the contributing role of skin-homing $\gamma\delta$ T cell subset has been demonstrated as well (6-10). In mouse models of skin inflammation and PV, peripheral γδ T cells colonize challenged dermis in increased numbers (6, 11), mediating enhanced effector functions (6, 7, 12-16) and an exacerbated inflammatory response with systemic effects (12, 17, 18). In humans, γδ T cells are rapidly recruited into physically perturbed skin (8), and their numbers are significantly altered in both the skin (6) and blood of PV patients (9, 10). However, the intrinsic changes that underlie shifts in their phenotypic and functional features or their T-cell receptor (TCR) repertoire in PV are still poorly understood and seldom addressed (10, 19, 20).

In healthy adults, the circulating $\gamma\delta$ T cell pool is predominantly populated by Vδ2 expressing cells with conserved Vγ9 chain pairing; in contrast, $V\delta 2^-$ cells, especially the $V\delta 1^+$ subset, are enriched across tissues (21). Rare populations expressing V δ 3–8 further complement the diversity of the human Vδ2 T cell compartment, particularly in the liver, jejunum, spleen and lung (21, 22). V γ 9V δ 2 cells exhibit a predominantly innate-like biology with constrained length and limited diversity of the TCR complementarity determining region 3 (CDR3) (23), allowing a low degree of clonotypic plasticity against butyrophilin 3A1 (BTN3A1)-restricted microbial or self-derived phosphoantigens (pAg) (24, 25). On the other hand, $V\delta 1^+$ lymphocytes harbor individual, mostly private repertoires with greater diversity in CDR3 length and Vy-chain pairing (26), that typically expand and become more focused in response to acute viral infections (26, 27), reflecting the adaptive nature of their immunobiology. The numerical and clonotypic expansion of the $V\delta 1^+$ compartment is accompanied by a transition from the naïve (CD27hiCD45RA+) to the effector memory phenotype (CD27^{lo/neg}CD45RA+), characterized by increased proliferative capacity and TCR reactivity, altered homing ability, and acquisition of cytotoxic granzymes. These adaptive-like features of the peripheral Vδ1⁺ Tcell compartment develop upon transcriptional reprogramming analogous to antigen-driven CD8⁺ αβT cell differentiation (28), with significant enrichment in genes linked to cytotoxicity, antigen processing and presentation, TCR/co-stimulatory receptors and IFN- γ response. Unlike V $\delta 1^+$ T cells, the adult V $\gamma 9^+$ V $\delta 2^+$ T lymphocytes acquire the innate-effector programming from early life onward (28), featuring central memory phenotype (CD27+CD45RA-), and semi-invariant TCR repertoire with largely public CDR3γ9 clonotypes (23, 28, 29).

Changes in the peripheral $\gamma\delta$ T cell composition, differentiation and TCR repertoire are also driven by sex (30, 31), age (32, 33) and latent CMV infection (34). In line, significantly lower percentages of $\gamma\delta$ T cell have been found in older, healthy male versus healthy female comparisons (31). Healthy aging alone induces a significant shift from naïve to late-stage effector phenotype in CMV-, and even more so in CMV⁺ individuals (34), driving numeric (35) and clonal expansion of $V\delta 1^+$ (27) and less abundant, adaptive-like $V\gamma 9^-V\delta 2^+$ pool (23). The predominant Vγ9/Vδ2 usage in young individuals is, moreover, significantly skewed toward Vγ2/Vδ1 specificity and increased Vγ2-8 gene usage in memory $\gamma\delta$ T cell compartment of healthy elderly, underlying significant functional and clonotypic alterations of $\gamma\delta$ T cell subsets with age. Similar studies in PV settings are, however, completely missing. To date, reduced numbers of circulating Vγ9Vδ2 T cells expressing skin-homing cutaneous lymphocyte-associated antigen (CLA) (8), and genes controlling IFN-γ/TNF signaling, T cell activation, and proliferation have been found in PV patients (19), and their transition from naïve to terminally differentiated phenotype has been linked to disease severity (19). Previously we reported that the proportions of other, sparsely represented $V\delta2^+ \gamma\delta TCR^{high}$ and $V\delta1^$ δ2- γδTCR^{int} cells were, in a converse fashion, increased selectively in male PV patients (9), and their peripheral perturbations were linked to altered mRNA/miRNA transcriptional circuits (10). The γTCR repertoire in psoriatic skin lesions has been described as highly polyclonal, private and largely devoid of dominant clonotypes (36), suggesting infiltration of diverse, unexpanded γδ T cell populations. However, the modulating effects of sex, age and CMV serostatus on the abundance, phenotype, or δTCR repertoire of γδ T cells in blood and skin of PV patients, have been largely overlooked.

To address this gap, we performed a bulk-TCRSeq and RNASeq analysis of the peripheral $\gamma\delta$ T cell repertoire and immunotranscriptome. Our data reveal that psoriasis drives profound, multifactorial changes in $\gamma\delta$ T cell repertoire and transcriptome. These alterations reflect the combined effects of chronic inflammation, aging, disease severity, and sex, contributing to extensive $\gamma\delta$ TCR repertoire attrition and skewing of the immune landscape toward oligoclonality, potentially impairing immunological responsiveness in psoriatic patients. The discovery of a functionally distinct, pro-inflammatory $\gamma\delta$ T cell subset and the identification of public but non-exclusive clonotypes provide a foundation for future research into their roles as biomarkers or therapeutic targets in psoriasis.

2 Materials and methods

2.1 Subjects

A total of 65 patients with clinically and histopathologically confirmed psoriasis vulgaris (PV) and 35 age- and sex-matched healthy controls were enrolled at the Department of Dermatology and Venereology, University Hospital Osijek, during routine diagnostic procedures. Disease severity and its impact on quality of life were evaluated using the Psoriasis Area Severity Index (PASI) and the Dermatology Life Quality Index (DLQI). The control group comprised unrelated adults with benign, non-infectious, and non-

allergic skin conditions. Exclusion criteria included infectious, autoimmune, or malignant diseases, recent allergic reactions (within six weeks before diagnostic procedures), and current systemic or phototherapy treatments. All individuals provided written informed consent.

Peripheral blood and skin biopsy samples were collected along with demographic, anthropometric, and detailed medical history data. Laboratory assessments included complete blood count, inflammatory markers (hsCRP, ESR), lipid profile, and serological markers for *Mycobacterium tuberculosis* (QuantiFERON-TB Gold test), hepatitis B (anti-HBs, HBsAg, anti-HBc IgG/IgM, HBeAg, anti-HBe), hepatitis C (anti-HCV), and cytomegalovirus (anti-CMV IgG/IgM). The study was approved by the Ethics Committee of the Faculty of Medicine in Osijek (Certificate No. 2158-61-07-19-126, October 11, 2019) and the Ethics Committee of the Clinical Hospital Centre Osijek (Certificate No. R2-12487/2019, September 12, 2019).

2.2 Peripheral blood mononuclear cell isolation, cryopreservation, and thawing

Peripheral blood mononuclear cells (PBMCs) were isolated from 20 mL of heparinized blood, diluted with 0.9% NaCl (1:1), and layered onto Lymphoprep (Stemcell Technologies, Vancouver, Canada) for density gradient centrifugation (800 x g, 25 min, no brake). The PBMC layer was harvested, washed with PBS, pelleted (400 x g, 10 min) and counted using the LUNA-II Automated Cell Counter (Logos Biosystems, South Korea) with Trypan blue staining. Cells were pelleted again and resuspended in cold cryopreservation medium [10% DMSO, 90% FBS (Sigma Aldrich, Germany)], at $4-5 \times 10^6$ cells per aliquot. Cryovials were stored at -80°C in a controlled-rate freezing container (Mr. Frosty, Nalgene) for 48 hours before transfer to liquid nitrogen. For thawing, PBMCs were rapidly warmed in a 37°C water bath and resuspended (1:4) in pre-warmed (37°C) supplemented RPMI-1640 medium [10% FBS, 1% sodium pyruvate (Capricorn Scientific, Germany), and 0.01M HEPES (Sigma Aldrich, Germany)]. The cells were then centrifuged ($350 \times g$, 5 min), resuspended in 5 mL of MACS buffer (PBS, 0.075% EDTA, 0.05% BSA), and analyzed for count and viability using the LUNA-II Automated Cell Counter.

2.3 Isolation of total leukocytes from skin

Total leukocytes were extracted from skin tissue using the Whole Skin Dissociation Kit (Miltenyi Biotec, Germany), which combines enzymatic digestion with mechanical dissociation. Skin biopsies were minced and initially passed through a 70 µm strainer to collect free cells. The remaining tissue fragments were then incubated with buffer L and enzymes D and A at 37°C for 3 hours, and afterwards homogenized using the MACS Dissociator (program h_skin_01). The homogenate was filtered through a 70 µm strainer and pooled with the previously collected cells. To maximize cell yield, the original MACS tube was rinsed with cold medium, and the rinse was also filtered into the same collection tube. The pooled suspension was then centrifuged (300 x g, 10

minutes, 4°C), resuspended in 3 mL of medium and counted using the LUNA-II Automated Cell Counter with Trypan blue exclusion. Finally, cells were pelleted again (350 x g, 5 minutes) and cryopreserved at 1 x 10^6 cells/mL, as described in section 2.2.

2.4 $\gamma\delta$ T cell immunophenotyping and sorting

Cryopreserved PBMCs were used for γδ T cell immunophenotyping and sorting. γδ T cells were identified using CD3 and pan-γδTCR antibodies, while $V\delta2^+$, $V\delta1^+$, and $V\delta1^-V\delta2^-$ subpopulations were distinguished using TCRV 82 and TCRV 81 antibodies (Supplementary Table 1). For immunophenotyping, 0.5×10^6 cells were stained with 0.25 µL of Live/Dead Fixable Near-IR Dead fluorescent dye (ThermoFisher Scientific, USA) for 15 min at 4°C in the dark, washed with PBS, pelleted (350 × g, 5 min), and incubated with 2.5 μL of TruStain FcX (BioLegend, USA) for 10 minutes at room temperature. Antibodies against CD3, γδ TCR TCRVδ1, and TCRVδ2 were then added for 30 minute γδ T cell staining (Supplementary Figure 1), followed by two PBS washes (350 \times g, 5 min). Samples were acquired on a BD FACS Canto II cytometer (Becton Dickinson, San Jose, CA, USA), with gating optimized using fluorescence-minus-one (FMO) controls, and compensation set with single-stained controls. Data were analyzed using the OMIQ Platform (Dotmatics, USA), and representative gating strategies are shown in Supplementary Figures 1A, B. Only samples with > 90% PBMC viability and > 50% skin lymphocyte viability were included (median viability was 98.7% (IQR: 97.28-99.5%) for PBMCs and 69.7 (58.8 - 84.6%) for skinderived lymphocytes).

For γδ T cell purification, two-way fluorescence-activated cell sorting (FACS) was performed using a Bio-Rad S3e cell sorter (Bio-Rad Laboratories, USA). On average, 13.6×10^6 thawed PBMCs (range: $5.65 \times 10^6 - 24.4 \times 10^6$) were processed per sample, yielding a median of 142,591 purified γδ T cells (IQR: 71,655 – 249,979). The staining protocol mirrored that of flow cytometry, except for the viability staining, which was validated using same samples processed in parallel for both methods. Sorted $\gamma\delta$ T lymphocytes were collected directly into 500 µL of TRI reagent (Sigma Aldrich, Germany) for immediate RNA extraction with Direct-zol RNA MicroPrep Kit (Zymo Research, USA). RNA quantity was assessed using the DeNovix QFX Fluorometer (DeNovix Inc., USA) and the Qubit RNA High Sensitivity Assay kit. Sorting accuracy and purity were assessed in PBMC samples of five randomly selected blood donors by flow cytometry (DxFLEX, Beckman Coulter, USA), with median purity of the sorted γδ T cell populations exceeding 95% (95.62% (IQR: 89.33% - 96.95%)).

2.5 Bulk-RNAseq analysis of peripheral $\gamma\delta$ T cell immunotranscriptome

A total of 24 $\gamma\delta$ T cell libraries (12 control, 12 patient) were prepared using the AmpliSeq for Illumina Immune Response Panel, following the manufacturer's protocol (Reference Guide v06, February 2019). In brief, libraries were generated through reverse transcription

(20 ng RNA), multiplex PCR amplification of 395 gene targets (19 cycles), FuPa digestion, adapter ligation with AmpliSeq TM UD Indexes, and magnetic bead–based purification (MagSi-NGSPREP Plus, MagnaMedics Diagnostics B.V., Netherlands). Refined libraries were amplified in the second amplification step (7 cycles), followed by tworounds of library cleanup. Libraries were quantified using KAPA Library Quantification Kit for Illumina platforms (Kapa Biosystems, USA) on a QuantStudio 5 system (ThermoFisher Scientific, USA) and assessed for fragment size (~300 bp) via agarose gel electrophoresis (1.5% gel, 150 V, 25 min). Libraries were diluted to 2 nM, pooled, denatured with 0.2 M NaOH, and sequenced on the Illumina MiniSeq platform (paired-end 2 × 150 bp) with 1% PhiX spike-in. Sequencing quality was assessed using Sequencing Analysis Viewer (SAV) v2.1 (Illumina, USA).

FASTQ reads were imported into the Galaxy platform, where FastQC was used for quality control. Reads shorter than 20 bp or with a quality score below Q20 were removed using Cutadapt. Remaining reads were aligned to the GRCh38 reference genome (UCSC Genome Browser), using the STAR aligner. Gene counts were obtained using FeatureCount, and differential gene expression (DEG) analysis was performed with the DESeq2 R package. Low-abundance transcripts with fewer than 10 reads in at least five samples per group (PV or HC) were excluded. Gene ontology and gene set enrichment analyses were performed with the clusterProfiler, AnnotationDbi, and msigdbr packages, while results were visualized with ComplexHeatmap, enrichplot, pathview, and ggplot functions.

2.6 Bulk-TCRSeq of peripheral blood $\gamma\delta$ T cells and skin-derived leukocytes

Libraries targeting CDR3 regions of γ - and δ -TCR chains were prepared using the Archer[®] ImmunoverseTM-HS TCR kit (Archer[®]Dx, USA), following the manufacturer's protocol. A total of 72 RNA samples were used, including 40 from sorted peripheral blood γδ T cells and 32 from skin-derived leukocytes, of which 10 were paired. Library preparation began with TCR-specific RT priming of 50 ng total RNA, followed by two-step cDNA synthesis. Libraries underwent end repair, AMPure bead-based purification, and two-step ligation with MBC adapters containing a P5 index, with unligated adapters removed via dual bead-based purification. Library enrichment included two PCR rounds: the first amplified TCR sequences with gene-specific primers, and the second added P7 indexes, with bead-based (MagSi-NGSPREP Plus) purification between rounds. The final libraries (~300 bp) were validated via electrophoresis, quantified by qPCR (KAPA Library Quantification Kit), normalized to 2 nM and sequenced on the Illumina NextSeq platform (paired-end 2 x 150 bp) with 20% PhiX spike-in.

2.7 TCR sequencing quality control and data pre-processing

TCR sequences were aligned, error-corrected, and CDR3 regions reconstructed using MiXCR (v.4.6.0.) (37). To ensure data

reliability, four peripheral blood and twelve skin-derived γδTCR libraries were excluded due to low sequencing depth, limited repertoire size, or disproportionate TRA/TRB vs. TRG/TRD read counts. Specifically, excluded samples included one blood library with extremely low read count (26 reads vs. a median of 1,001,089), four skin samples lacking TRG and/or TRD sequences, one blood (7 clonotypes vs. a median of 1,548) and eight skin samples (≤ 10 clonotypes vs. a median of 108.5) with very low TRG/TRD clonotypes, and two blood libraries with disproportionately high TRA/TRB transcript proportions (91.1% and 66.7% vs. a median of 12.5%). Sequencing depth generally did not correlate with clonotype counts, except for a significant correlation between skin TRD read counts and clonotype numbers ($\rho = 0.621$, P = 0.003), suggesting partial under-sampling of skin TRD repertoires. Detailed sequencing metrics of blood and skin TRG and TRD repertoire are provided in Supplementary Table 2 -Supplementary Table 5.

MiXCR clonotype tables were next converted to VDJTools format, filtered to remove erroneous and non-functional clonotypes, and corrected by merging low-abundance clonotypes with similar, highabundance ones, reducing sequencing and PCR errors. Pseudogenes (e.g., TRGV10), and TRAV-incorporating variants were also excluded, retaining only functional TRG (TRGV2, TRGV3, TRGV4, TRGV5, TRGV8, TRGV9) and TRD (TRDV1-TRDV8) segments. This filtering preserved > 95% of sequencing reads (blood: 99.1 ± 1.9% of TRD and 97.5 \pm 4.1% of TRG; skin: 95.17 \pm 6.96% of TRD and 99.7 \pm 0.77% of TRG). Final datasets included 1.73×10^7 TRG and 8.85×10^6 TRD blood-derived sequences, and 6.01 x 10^5 TCR γ and 1.58 x 10^5 TCR δ cutaneous sequences. The average reads per sample were 4.95 x 10⁵ TRG and 2.53×10^5 TRD in blood, and 2.4×10^4 TRG and 7.89×10^3 in skin (Supplementary Table 4 and Supplementary Table 5). The average number of unique clonotypes in blood samples was 928 (minmax:122-2292) for TRG and 933 (min-max: 76-2176) for TRD, while in skin samples the averages were 73 (19-182) for TRG and 19 (6-56) for TRD (Supplementary Table 4 and Supplementary Table 5).

2.8 TCR γ and TCR δ repertoire analysis

TRG and TRD repertoires were subsequently analyzed using VDJTools (38) and the Immunarch R package (39). CDR3γ and CDR38 clonotypes were classified by TRGV and TRDV variants, focusing on the most prevalent TRDV (TRDV1, TRDV2, TRDV3) and coding TRGV segments (TRGV2, TRGV3, TRGV4, TRGV5, TRGV8, TRGV9). Basic repertoire metrics (read counts, clonotype numbers, CDR3 length), were obtained using the CalcBasicStats command. Clonotype frequencies were normalized within each TRGV and TRDV category to sum to 1, ensuring diversity assessments were independent of their overall contribution to the total repertoire. Gene segment usage and CDR3 length distributions were assessed with CalcSegmentUsage and CalcSpectratype, respectively. V-J pairing frequencies were visualized with PlotFancyVJUsage. Diversity indices (D50, Chao1, Efron-Thisted estimate, inverse Simpson and Shannon-Wiener index) were computed using CalcDiversityStats. Shared clonotypes were identified using JoinSamples, while inter-sample similarity was

assessed with Immunarch's *repOverlap*, calculating the Jaccard index. Additional trends in CDR3 length and gene usage were explored with *repExplore* and *trackClonotypes*, respectively. For age-associated correlation analyses in peripheral repertoires, the four oldest PV patients were excluded to avoid interpretation bias due to the absence of age-matched healthy controls.

3 Results

3.1 Subject characteristics and $\gamma\delta$ T cell immunophenotypic profiles in psoriasis versus healthy controls

The basic characteristics of the study participants are listed in Table 1. Psoriasis patients (PV) and healthy controls (HC) were well matched for sex and age, though PV patients had modestly higher BMI. Most PV participants had moderate-to-severe disease with a disease duration of 9 years. In peripheral blood, leukocyte counts were elevated in PV, whereas hsCRP levels did not differ between groups. CMV seroprevalence was high in both groups, consistent with trends in Croatian population (40), though rates were slightly lower in PV. In contrast, anti-HBs seropositivity was markedly reduced in PV compared to HC (20/42 vs. 16/14; $P = 2.2 \times 10^{-16}$), likely reflecting differences in prior vaccination under Croatia's mandatory HBV immunization program. Flow cytometry revealed no significant case-control differences in the overall frequency of circulating $\gamma\delta$ T cells, or their major subsets $(V\delta1^+, V\delta2^+, \text{ or } V\delta1^-$ Vδ2⁻). However, sex-stratified analysis revealed a selective reduction in total $\gamma\delta$ T cells and the $V\delta2^+$ subset in male PV patients compared to healthy male controls (Supplementary Figure 2). This finding is consistent with prior reports of diminished peripheral Vγ9Vδ2 T cells in psoriasis (8, 19), but here points to a male-specific effect. However, healthy female controls in our cohort displayed inherently lower proportions of $\gamma\delta$ T (median 3.11% [2.48 – 3.91] vs. 5.18% [3.07 – 7.46] in males, P = 0.028) and $V\delta 2^+$ cells (1.57% [1.37 – 2.42] vs. 3.37 [1.93 – 6.68] in males, P = 0.018) compared to healthy males, potentially masking disease-associated alterations in unstratified comparisons. Frequencies in female PV patients did not differ significantly from healthy females or affected males, suggesting sex-specific γδ T cell dynamics that warrant further study in larger, sex-balanced cohort. In psoriatic lesions, CD3+T cells were significantly enriched compared to healthy skin (Supplementary Figure 3A), consistent with infiltration of T cells in inflamed skin. Within the $\gamma\delta$ T cell compartment, the V\delta1^-V\delta2^- subset was significantly expanded in PV skin (Supplementary Figure 3B). Intriguingly, female patients showed a progressive expansion of Vδ2⁺ cells with increasing PASI scores ($\rho = 0.846$, P = 9.7 x 10^{-4}), while overall $\gamma\delta$ T cell frequencies in psoriatic skin declined sharply with age ($\rho = -0.722$, P = 9.83 x 10⁻⁸), accompanied by reduced frequencies of the Vδ1 subset ($\rho = -0.401$, P = 0.009). These associations were absent in healthy participants, suggesting disease-associated remodeling of $\gamma\delta$ T cell subsets.

3.2 Distinct alterations in $\gamma\delta$ TCR gene segment usage between blood and skin of psoriatic patients

The composition of blood and skin $\gamma\delta$ TCR repertoires was first assessed by analyzing TRGV/TRGJ and TRDV/TRDJ gene segment usage. As expected, TRGV9 and TRDV2 segments dominated the peripheral blood, accounting for over 80% of clonotypes. The most prevalent variants featured canonical TRGV9-TRGJP and TRDV2-TRDJ1 rearrangements, aligning with prior findings [1–3]. While these clonotypes dominated most blood samples, alternative TRG and TRD rearrangements were also observed across individuals (e.g. TRGV9-TRGJ2, TRGV4-TRGJ2, TRDV1-TRDJ1, TRDV2-TRDJ3), in some cases at frequencies comparable to canonical pairings (Figures 1A, B, Supplementary Figures 4A, B). However, these variations in the peripheral blood $\gamma\delta$ TCR repertoire were not associated with disease status, as no significant differences were observed in TRG or TRD gene segment usage between healthy and

TABLE 1 Baseline subject characteristics and distribution of $\gamma\delta$ T cell subsets in blood and skin.

| | PV | HC | Р |
|--|-----------------------------|--------------------------|---------|
| Age | 44 (33 – 57) | 37 (31 – 47) | 0.137* |
| Sex (M/F) | 49/16 | 25/10 | 0.812** |
| BMI | 30.12 (25.23 – 32.79) | 27.14 (25.82 – 29.33) | 0.048* |
| hsCRP (mg/L) | 1.60 (0.68 – 3-91) | 1.38 (0.70 - 2.40) | 0.603* |
| L (N x10 ⁹ /L) | 7.4 (6.40 – 9.50) | 6.4 (5.15 – 7.05) | 0.001* |
| CMV IgG (U/mL) | 97.85 (45.45 – 129) | 108 (89.95 – 130) | 0.214* |
| CMV IgG (pos/neg) | 49/13 | 29/1 | 0.031** |
| PASI | 16.1(7.15- 22.25) | - | - |
| Disease duration (years) | 9 (5 – 17) | - | - |
| % γδTCR ⁺ of CD3 ⁺ in PB | 6.85 (3.96 – 9.5) | 6.34 (4.75 - 8.23) | 0.764* |
| % V $\delta2^+$ of $\gamma\delta$ T in PB | 68.8 (51.4 - 85.4) | 66.4 (48.2 - 81.3) | 0.667 * |
| % $V\delta 1^+$ of $\gamma\delta$ T in PB | 21.1 20.4 (10.75– 32.58) | 26.2 (14.3 - 41.6) | 0.251* |
| %V δ 1 V δ 2 of $\gamma\delta$ T in PB | 4.39 (2.32 – 12.9) | 3.92 (2.18 – 11.4) | 0.598* |
| % γδTCR ⁺ of CD3 ⁺ in skin | 1.25 (0.77 – 1.62) | 1.76 (1.20 – 2.58) | 0.065* |
| % V $\delta 2^+$ of $\gamma \delta$ T in skin | 23.5 (16.3 – 36.9) | 22.7 (14.13 – 53.08) | 0.669* |
| % V δ 1 $^+$ of $\gamma\delta$ T in skin | 36.6 (29 – 60.5) | 46.1 (31.33 – 61.03) | 0.461* |
| %Vδ1 Vδ2 of γδ T in skin | 23.7 (18.1 – 38.9) | 17.7 (8.96 – 27.5) | 0.029* |

Continuous data are shown as median (interquartile range). BMI, body mass index, hsCRP, high sensitivity C, reactive protein, L, leukocyte count, CMV, cytomegalovirus; PASI, psoriasis area and severity index; PB, peripheral blood. * Mann-Whitney U test, ** Fisher's Exact Test. Bold values indicate P < 0.05.

psoriatic individuals (Figure 1C, Supplementary Table 6 and Supplementary Table 7).

The cutaneous TCRy repertoire displayed a more balanced distribution among TRGV2-TRGV9 variants (Figure 1D, Supplementary Figure 4C), contrasting the dominance of TRGV9-TRGJP clonotypes in blood. In skin, TRG clonotypes preferentially rearranged with non-TRGJP variants, with TRGJ2 being the most abundant, followed by TRGJP2 and TRGJP1. Similarly, while TRDV2 clonotypes dominated the peripheral blood, the cutaneous repertoire displayed a more equal representation of TRDV1 and TRDV2, with a smaller contribution from TRDV3 clonotypes (Figure 1E, Supplementary Figure 4D). Notably, psoriatic lesional skin displayed nominal TRGV9 enrichment (Figure 1F 25.94% vs. 12.6%, P = 0.034), and TRDV3 depletion (Figure 1F; 4.34% vs. 20.28%, P = 0.038) compared to healthy skin; however, these trends did not remain statistically significant following multiple testing correction (Benjamini-Hochberg, Supplementary Table 8 and Supplementary Table 9). Beyond group comparisons, repertoire features were associated with disease severity and age. In lesional skin, TRGV8 clonotype proportions decreased significantly with increasing disease severity ($\rho = -0.736$, P = 0.003), while TRGV2-TRGJP1 transcripts positively correlated with PASI ($\rho = 0.85$, P = 0.006). Conversely, in peripheral blood, TRGV2-TRGJP1 clonotypes declined with patient age (Figure 1G), paralleling the age-related decline in blood TRGV8-TRGJ2 clonotypes (Figure 1H). Notably, this trend was reversed in diseased skin, where TRGV8-TRGJ2 clonotypes increased significantly with age (Figure 1H). Additionally, blood TRGV4 clonotypes showed a strong positive correlation with disease duration ($\rho = 0.63$, P = 0.003), driven primarily by the TRGV4-TRGJ2 rearrangement (Figure 1I). These age- and disease-associated shifts in γδTCR repertoire were absent in healthy individuals, who instead exhibited an age-associated increase in TRGV2-TRGJP1 clonotypes (Figure 1G).

Collectively, our findings reveal that psoriasis drives distinct alterations in the $\gamma\delta$ TCR repertoires of peripheral blood and skin, characterized by nominal TRGV9 enrichment and TRDV3 depletion in the skin, along with contrasting disease and agerelated patterns in TRGV2-TRGJP1 and TRGV8-TRGJ2 transcript abundance between these compartments compared to healthy controls.

3.3 Age, sex, and disease severity influence divergent CDR3 length dynamics in PV

We further evaluated the structural and functional properties of TCR γ (TRG) and TCR δ (TRD) repertoires, including CDR3 length distribution, convergence, and junctional diversity (nucleotide insertions, deletions, and nontemplated additions).

TRG clonotypes displayed a wide CDR3 length distribution ranging from 6 to 22 amino acids (Figure 2A). Among blood-derived clonotypes, roughly 70% measured between 13 and 17 amino acids (Figure 2A), whereas skin-derived clonotypes were significantly shorter, mostly falling within the 11–16 amino acid

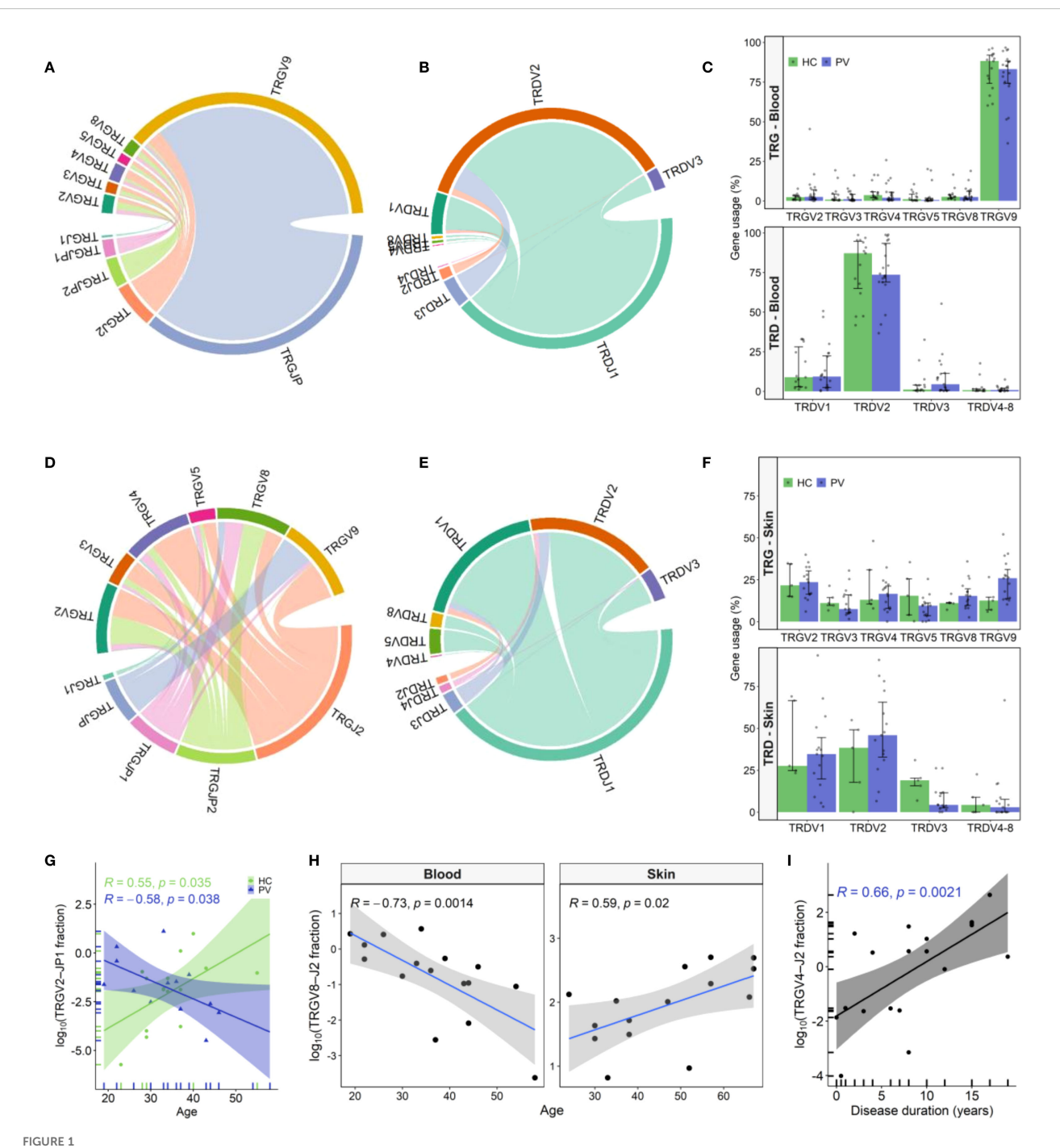
range (Figure 2A), indicative of tissue-specific differences in V-J gene usage. Circulating repertoires were primarily composed of TRGV9-expressing clonotypes (Figure 1A), which tend to have longer CDR3 regions (10-20 amino acids, Figure 2C), whereas skin repertoires were enriched for TRGV2/3/4/5/8 segments (Figure 1D), which typically generate shorter CDR3s (11-15 amino acids, Supplementary Figure 5). In addition, TRGV9 clonotypes in the skin primarily featured TRGV9-TRGJ2 rearrangements (Figure 2B), in contrast to the TRGV9-TRGJP rearrangements that dominated in the blood (Figure 2B), likely contributing to the shorter and bimodal TRGV9 CDR3 length distribution observed in the skin (Figure 2C). Conversely, TRGV2/3/4/5/8 lengths remained consistent across both compartments (Supplementary Figure 5). Bimodal distributions were also evident in the TRDV1 and TRDV3 (Figures 2D, E) repertoires from both blood and skin, whereas TRDV2 clonotypes exhibited a continuous CDR3 length range (Figure 2F). Of interest, longer TRDV1/2/3 clonotypes were largely absent in healthy skin compared to lesional skin (Figures 2D-F).

Although overall CDR3 length profiles did not differ dramatically between psoriasis patients and healthy controls, subgroup analyses revealed diverse trends in PV that were absent in HC. In patient blood, TRGV9 CDR3 lengths contracted with age, whereas TRDV1 lengths expanded (Figure 2G). Female PV patients exhibited longer CDR3δ2 regions than male PV patients (Supplementary Figures 6A, B) a sex difference not seen in HC (P = 0.845). In addition, their CDR3 δ 2 were also longer than those of healthy females (51.04 [50.64-51.24] nt vs. 49.28 [49.21-49.56] nt, P = 0.011), likely reflecting higher frequency of expanded TRDV2-TRDJ3 clonotypes in female patients, which are intrinsically longer than TRDJ1 or TRDJ2 counterparts (Supplementary Figures 6C, D). These sex-linked shifts in peripheral CDR3 length profile were not mirrored in skin. Disease severity positively correlated with TRGV8 CDR3 length in blood and skin (Figure 2H), and with increased nucleotide insert size in cutaneous TRD clones ($\rho = 0.578$, P = 0.026), particularly within TRDV2 clonotypes (Figure 2I). Finally, TCR convergence, defined as distinct nucleotide sequences encoding identical CDR3 amino acid sequence, declined with age in PV blood for both γ ($\rho = -0.55$, P = 0.028) and δ chains ($\rho =$ -0.69, P = 0.003), but not in age-matched HC.

Taken together, these results highlight that psoriasis is associated with subtle, yet significant remodeling of $\gamma\delta$ TCR structural and junctional diversity, modulated by age, disease severity, and sex.

3.4 Disease severity drives $\gamma\delta$ TCR repertoire contraction in psoriasis

To characterize the $\gamma\delta$ TCR repertoire diversity, we analyzed clonotype counts, diversity indices, and repertoire space distribution in blood and skin from PV patients and healthy controls. Blood clonotypes were grouped by frequency into 'hyperexpanded' (>5%), 'large' (0.5–5%), 'medium' (0.05–0.5%), and 'small' (<0.005%) compartments. In skin, the much lower



TRG and TRD gene usage patterns in peripheral blood and skin of psoriasis patients and healthy controls. (**A**, **B**) Chord diagrams from pooled peripheral blood $\gamma\delta$ T cell clonotypes from psoriasis vulgaris (PV; N = 20) and healthy controls (HC; N = 15) depict TRGV-TRGJ (**A**) and TRDV-TRDJ (**B**) rearrangements, with TRGV9-TRGJP and TRDV2-TRDJ1 being the most prevalent pairings. (**C**) TRGV and TRDV segment usage in blood did not differ between PV and HC. Bars represent median \pm IQR. (**D**, **E**) Chord diagrams from skin-derived clonotypes (PV: N = 15; HC: N = 5) demonstrate greater TRGV-TRGJ (**D**) and TRDV-TRDJ (**E**) diversity compared to blood, with increased usage of non-TRGV9 segments and a more balanced TRDV1/TRDV2 distribution. (**F**) In skin, TRGV9 usage is elevated and TRDV3 reduced in PV relative to HC, but differences did not remain significant after correction for multiple testing. Bars represent median \pm IQR. (**G**) Frequency of circulating TRGV2-TRGJP1 clonotypes declines with age in PV patients (N = 26) but increases with age in HC (N = 15). (**H**) TRGV8-TRGJ2 clonotypes decrease with age in blood of PV patients (N = 26) but increase in lesional skin (N = 15). (**I**) Circulating TRGV4-TRGJ2 clonotype frequency correlates positively with disease duration (N = 30). In all correlation plots, Spearman correlation coefficients (R) and p-values are indicated. In age correlation analyses (**G**-**H**), the four oldest PV participants were excluded due to lack of age-matched HC individuals.

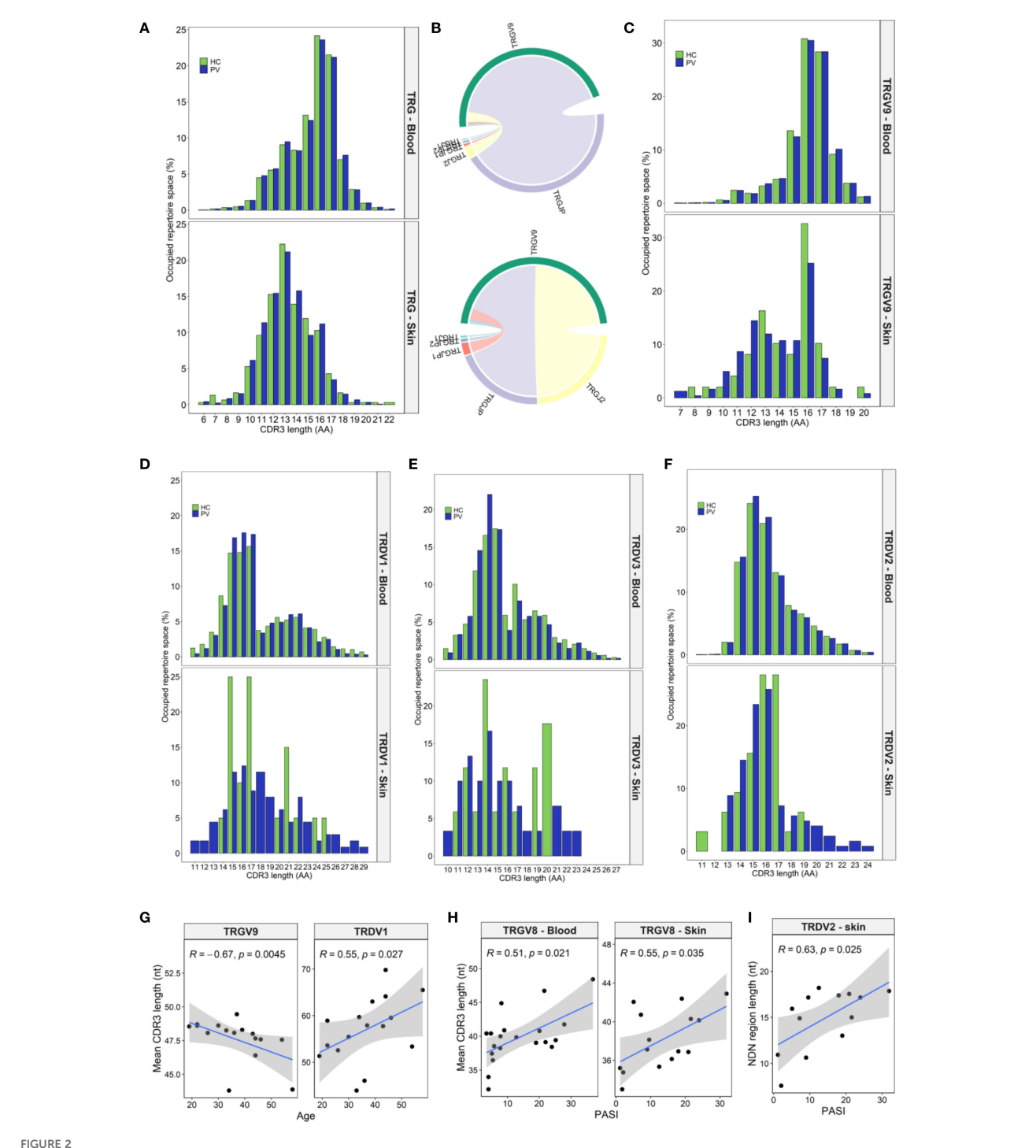


FIGURE 2
Tissue-specific and psoriasis-associated alterations in CDR3 length distributions of TRG and TRD clonotypes. (A) Spectratype analysis of TRG CDR3 length distributions in peripheral blood (PV: N = 20; HC: N = 15) and skin (PV: N = 15; HC: N = 5) reveals that circulating repertoires span a broader range (13–17 amino acids), while skin clonotypes show a narrower and shorter profile (11–16 aa). (B) Chord diagrams from pooled blood (N = 35) and skin (N = 15) TRGV9 clonotypes show dominant TRGV9–TRGJP pairings in blood and more balanced TRGV9–TRGJP and TRGV9–TRGJ2 usage in skin. (C) This recombinatorial difference underlies the bimodal CDR3 length distribution observed in skin TRGV9 clonotypes. (D-F) TRDV1 (D) and TRDV3 (E) display bimodal length patterns, while TRDV2 (F) demonstrates a continuous distribution. Longer CDR3 sequences within the TRDV repertoire are selectively depleted in healthy skin compared to lesional psoriatic skin. (G) In PV patients, TRGV9 CDR3 length in blood inversely correlates with age while TRDV1 CDR3 length increases with age. (H) TRGV8 CDR3 length positively correlates with Psoriasis Area and Severity Index (PASI) in both blood and skin. (I) Increased junctional (NDN) region length in skin TRDV2 clones also associates with higher PASI scores. Data in panels (A, C), and (D-F) presents median percentage of repertoire occupancy per CDR3 length bin. Panels (G-I) display Spearman correlation coefficients (R) with p-values. In age-related correlation analyses (G), four oldest PV donors were excluded due to lack of matched healthy controls.

read depth and clonotype counts (Supplementary Table 5) necessitated a simplified scheme: TRG clonotypes were assigned to 'hyperexpanded', 'large', or 'medium' groups, while TRD clonotypes were too sparse for frequency-based partitioning. Repertoire diversity was in addition evaluated using the Efron-Thisted and Chao1 estimators (to capture rare variants), Shannon-Wiener and Inverse Simpson indices (to assess overall richness and evenness), and the D50 index (to quantify clonal expansion).

Overall, total blood TCRγ and TCRδ clonotype counts and diversity indices were similar between PV patients and healthy controls (Supplementary Table 10). However, increasing PASI scores were associated with a marked contraction of circulating y and δ clonotypes (Figure 3A), contrasting increasing fraction of cutaneous TRG/TRD reads with both disease duration and severity (Figure 3B). The most pronounced PASI-dependent decreases in the blood repertoire were observed for the TRGV9 and TRDV2 subsets (Figure 3C). This loss of blood repertoire richness was driven by depletion of rare ('small') clonotypes and was mirrored by reduced Chao1 and Efron-Thisted diversity estimates (Supplementary Table 11). Concurrently, the 'hyperexpanded' TRG compartment increased (Supplementary Table 11), indicating a PASI-associated shift toward clonal expansion. Peripheral diversity losses associated with PASI were also observed across TRGV2, TRGV4, TRGV8, and TRDV3 subsets (Supplementary Table 11), highlighting that disease severity impacts multiple γδ T cell subsets.

In lesional skin, TRGV8 representation within 'large' and 'hyperexpanded' fractions declined with PASI (Figure 3D), paralleling elevated peripheral TRGV8 D50 values (Figure 3E). Disease duration further remodelled the repertoire architecture. In blood, TRGV4 clonotypes showed lower D50 over time (Figure 3F), with concomitant enrichment in the 'large' frequency compartment (Figure 3G), while the medium-frequency TRGV4 clonotypes increased in the skin (Figure 3H). Similarly, prolonged disease reshaped the 'small' TRD compartment in blood, marked by TRDV2 depletion ($\rho = -0.46$, P = 0.041) and reciprocal TRDV1 enrichment ($\rho = 0.48$, P = 0.033).

Collectively, these findings demonstrate that PV severity selectively contracts the peripheral $\gamma\delta$ TCR repertoire while reshaping lesional skin subsets, pointing to compartment-specific alterations that may contribute to local inflammation and systemic immune modulation.

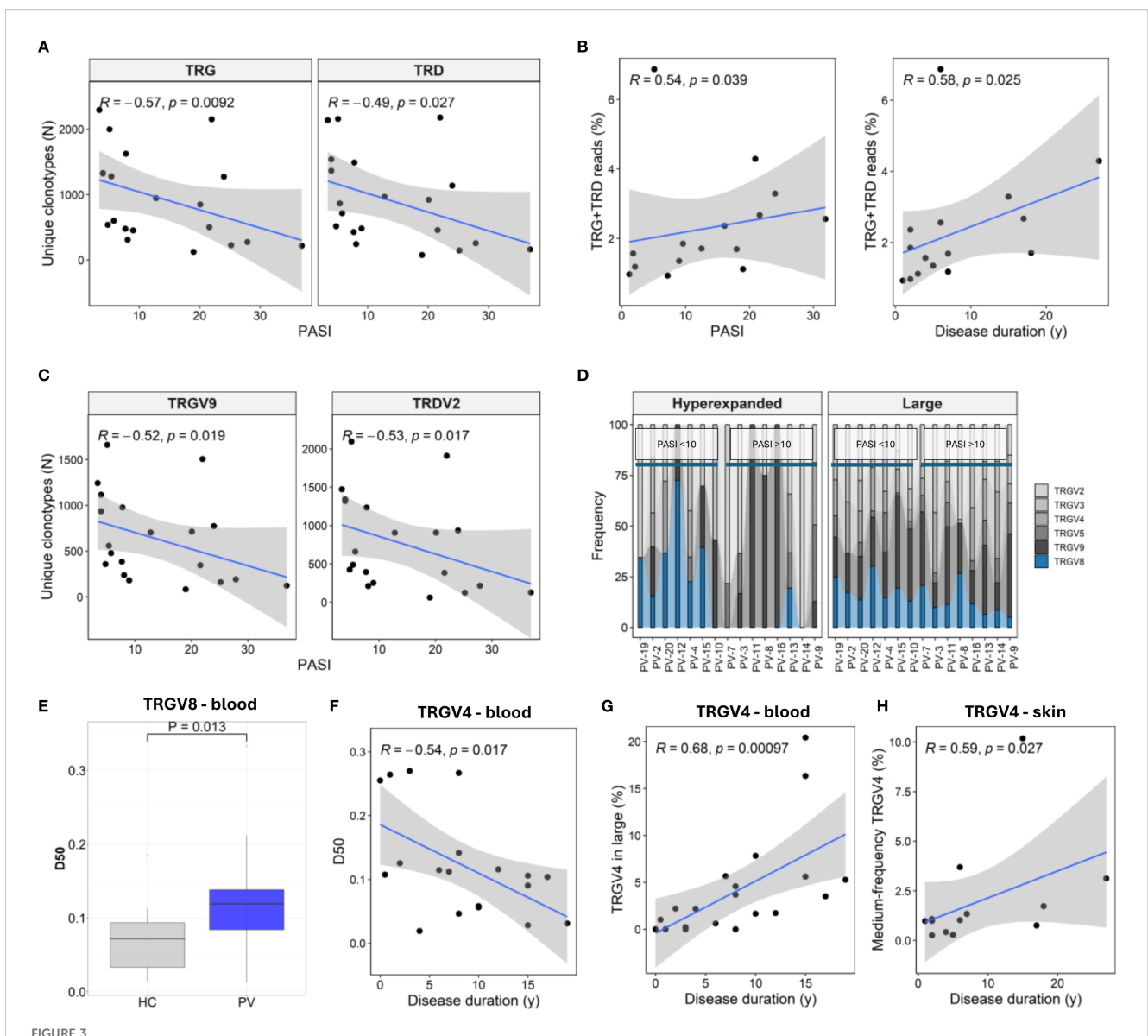
3.5 Age-driven peripheral $\gamma\delta$ TCR contraction outpaces effects of disease severity in psoriasis vulgaris

Owing to limited clonotype diversity in skin, we further focused on the $\gamma\delta$ TCR repertoire in peripheral blood, where age-related effects paralleled, and often exceeded, those associated with PASI. In PV patients, advancing age correlated with dramatic reductions in total TCR γ and TCR δ (Figure 4A) clonotype counts, driven by loss

of the 'small' and 'medium' TRG and TRD clonotype compartments (Figure 4B, C), and the expansion of the 'hyperexpanded' clones (Figure 4B, D). These shifts were most pronounced in TRGV9 and TRDV2 and extended across TRGV2–8 and TRDV3 subsets, where the loss of small clonotypes was coupled with declines in several diversity indices (Supplementary Table 12).

In healthy controls, these age-associated γδTCR repertoire constrictions were absent (Figures 4E-H). Instead, older healthy controls displayed expansions of TRDV1 and TRGV2 clonotype count (Figures 5A, B), especially within the large-clone compartment (TRDV1: $\rho = 0.527$, P = 0.043, TRGV2: $\rho = 0.643$, P = 0.01), which correlated with CMV IgG titers (Figures 5C, D). In PV, CMV seropositivity further enriched TRDV1 in both 'small' ($\rho = 0.553$, P = 0.011) and 'large' clonotype compartments (Figure 5C), and deepened TRDV2 loss ($\rho = -0.529$, P = 0.017), highlighting a complex interplay of viral exposure, ageing, and chronic inflammation in PV. Importantly, flow cytometry confirmed that TRDV2 clonotype reductions reflected loss of clonotypic diversity rather than cell numbers, as blood V82+ frequencies did not vary with PASI ($\rho = -0.09$, P = 0.74) or age ($\rho = -0.36$, P = 0.17). Moreover, higher CMV IgG titers in PV patients were linked to reduced $V\delta 2^+$ frequencies ($\rho = -0.691$, $P = 7.38 \times 10^{-4}$) and expansion of the $V\delta 1^{-}V\delta 2^{-}$ subset ($\rho = 0.541$, P = 0.014) among total $\gamma\delta$ T cells, supporting the contribution of CMV on γδTCR repertoire reshaping. However, CMV IgG levels in PV did not correlate significantly with age $(\rho = 0.393, P = 0.086)$, disease duration $(\rho = -0.056, P = 0.815)$, or PASI $(\rho = 0.198, P = 0.404)$, indicating that CMV is unlikely a primary driver of age- and disease severity-associated repertoire changes.

To pinpoint drivers of clonal expansion, we analyzed the top 10 clonotypes. Their cumulative frequencies increased with PASI (TCRy: ρ = 0.542, P = 0.014; TCRδ: ρ = 0.457, P = 0.043) and age (TCR γ : ρ = 0.797, P = 2.2×10^{-4} ; TCR δ : $\rho = 0.673$, P = 0.004). Additionally, we summed the frequencies of the first 10 clonotypes within distinct TRDV and TRGV gene segments, independent of their position in the overall repertoire ranking. This revealed segment-specific associations: TRDV3 frequencies correlated with disease severity ($\rho = 0.517$, P = 0.023), TRDV2 with age ($\rho = 0.551$, P = 0.027), and TRGV4 with disease duration ($\rho = 0.470$, P = 0.037). Stratification by age (< 40 vs. \geq 40 years) and PASI (\leq 10 vs. > 10) further showed that older patients, but not those with higher PASI, harbor significantly higher cumulative frequencies of top clonotypes (TCRy: 83.4% vs. 30.7%, P = 0.008; TCRδ: 73.2% vs. 32.3%, P = 0.026). Patient age also correlated with longer CDR3 δ lengths ($\rho = 0.601$, P = 0.014) and increased NDN additions in non-TRDV2 clonotypes ($\rho = 0.613$, P = 0.034), with females exhibiting longer CDR3δ2 regions than males (48.1 [46.3 -49.8] vs 52 [50.8 - 52.9], P = 0.006; M vs F), patterns absent in controls. In summary, aging in PV patients triggers a pronounced contraction of peripheral γδTCR diversity alongside expansion of dominant clones, surpassing changes driven by disease severity. In contrast, healthy individuals exhibit CMV-associated repertoire expansions with age, whereas in PV the interplay of aging, CMV exposure, and chronic inflammation predominantly narrows γδTCR diversity without altering cell numbers.



Disease severity and duration shape TRG and TRD repertoires in blood and skin of psoriasis patients. (A) Circulating $\gamma\delta$ T cell repertoire diversity declines with increasing Psoriasis Area and Severity Index (PASI), as reflected in reduced numbers of unique TRG and TRD clonotypes (N = 30). (B) In lesional skin (N = 15), the proportion of TRG and TRD reads increases with both PASI and disease duration. (C) TRGV9 and TRDV2 clonotypes in peripheral blood (N = 30) show marked contraction with higher PASI scores. (D) TRGV usage within hyperexpanded and large frequency clonotype compartments in lesional skin shows decreased TRGV8 representation in patients with high PASI scores (PASI >10). (E) D50 values (fraction of clonotypes required to account for 50% of total reads) of TRGV8 clonotypes are elevated in PV patients. P-value calculated by Mann-Whitney U test. (F) TRGV4 repertoire diversity in blood declines with disease duration. (G) TRGV4 representation increases within the large frequency clones (0.5 – 5%) in blood. (H) The proportion of medium-frequency (0.5 – 5%) TRGV4 clonotypes increases with disease duration in lesional skin. Panels (A-C, F-H) show Spearman correlation coefficients (R) with associated p-values.

3.6 Peripheral $\gamma \delta TCR$ repertoires in psoriasis show polyclonal diversification and partial blood-skin sharing

Analysis of paired peripheral and cutaneous $\gamma\delta$ TCR repertoires revealed extensive diversity but limited disease-specific clonotypes in psoriasis. In blood, 27,073 TCR δ and 15,364 TCR γ clonotypes were identified (Supplementary Table 5), with markedly lower counts in skin (356 TCR δ ; 1,215 TCR γ). Most TCR δ clonotypes were private (7.5% public in blood; 0.84% in skin; Figures 6A-D),

whereas TCR γ repertoires were more public (18.8% and 10.29%, respectively; Figures 6E-H). Within the public blood compartment, TRDV2 dominated TCR δ and TRGV9 dominated TCR γ usage, with lower contributions from TRDV1/3 and TRGV2/3/4/5/8 (Supplementary Table 13). Although several clonotypes were enriched in PV or healthy donors, none reached statistical significance after Fisher's exact test with Benjamini-Hochberg correction. Jaccard index (JI) analysis showed reduced intra-PV overlap for TRGV8 (PV–HC overlap 0.009 [0–0.016], P = 0.002; Supplementary Figure 7A) and a similar but less pronounced

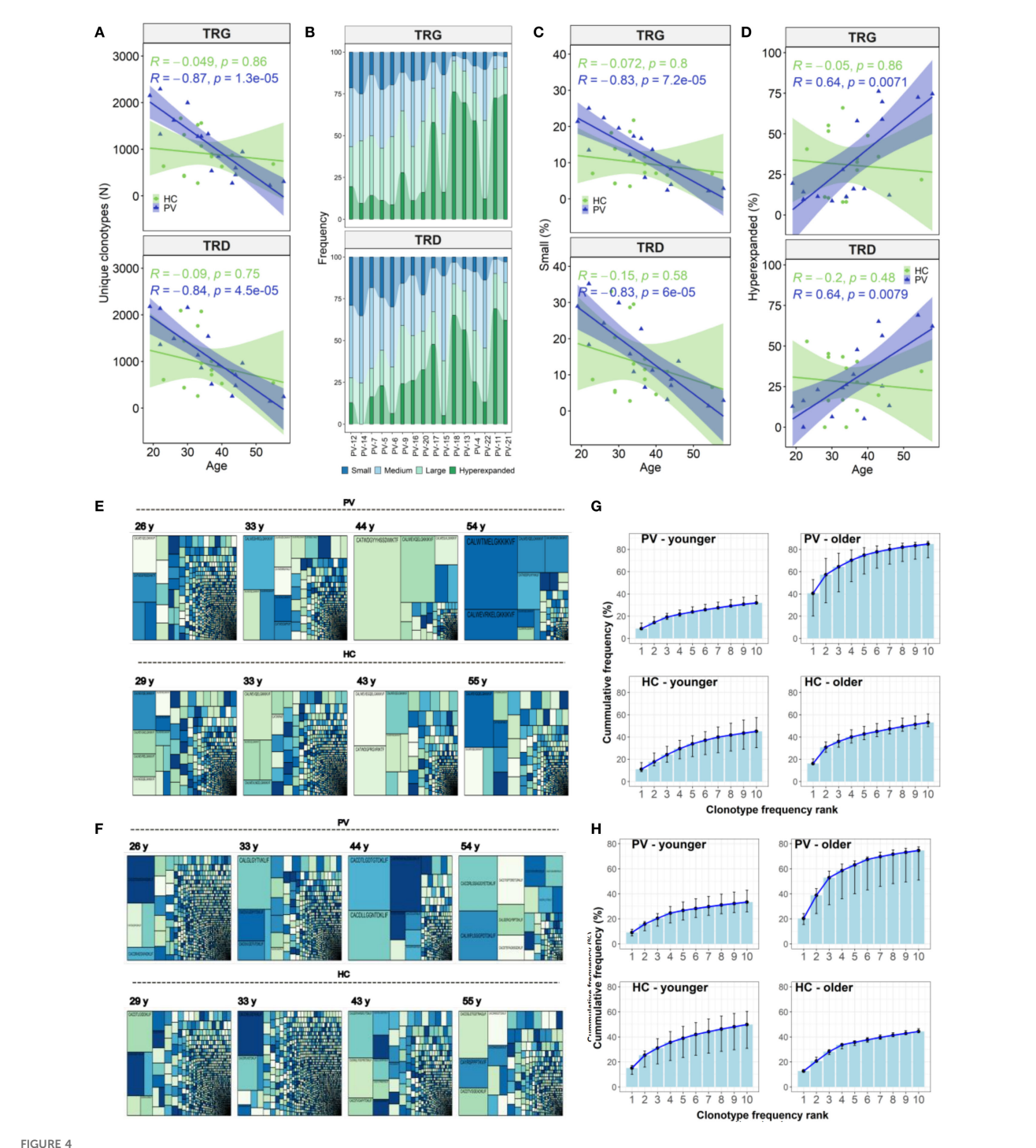
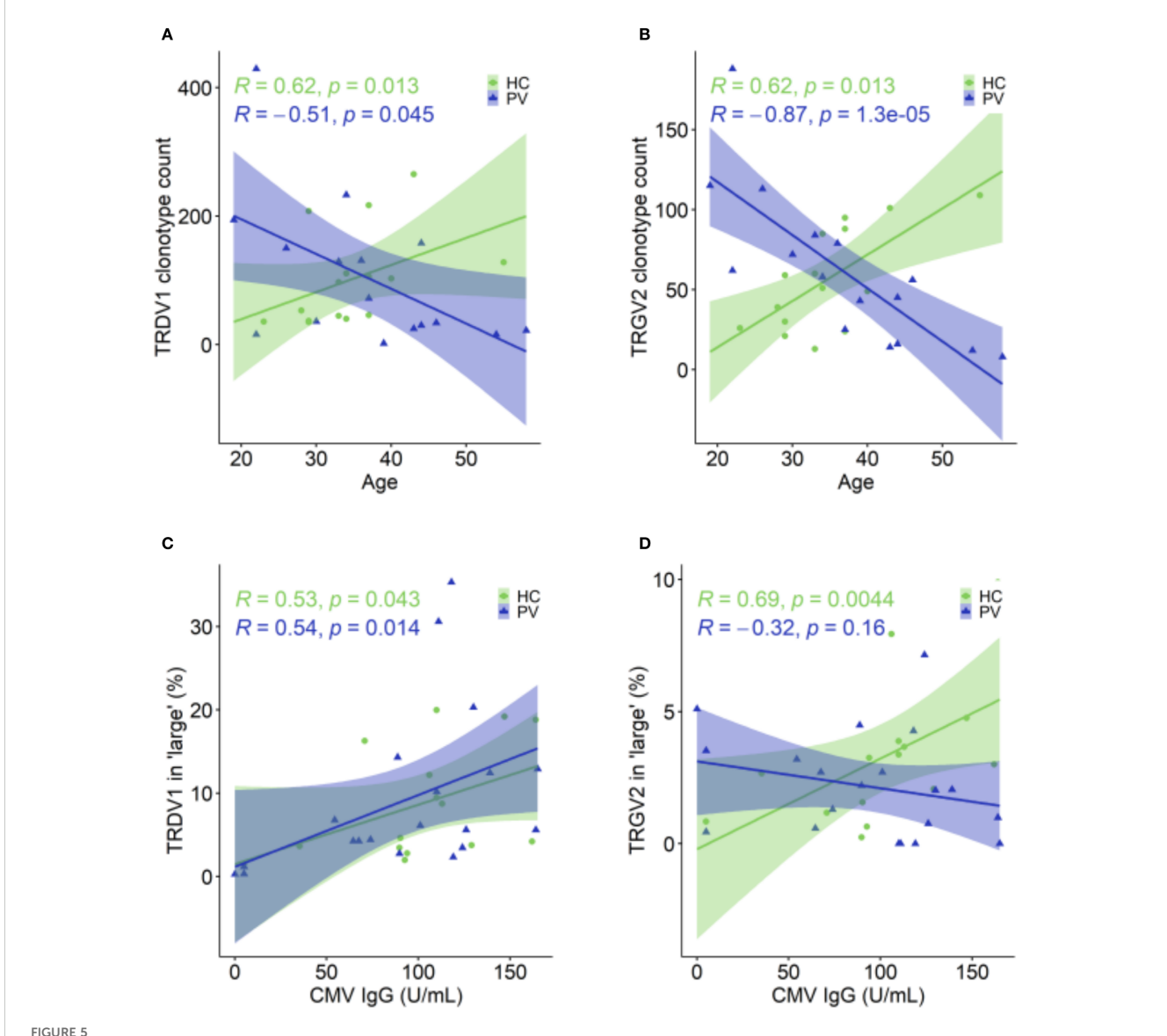


FIGURE 4
Age-related contraction of circulating $\gamma\delta$ T cell repertoires in psoriasis vulgaris. (A) Advancing age in PV patients (N = 26) is associated with a decline in the total number of unique TRG and TRD clonotypes in peripheral blood, a trend not observed in healthy controls (N = 15). (B) Clonotype abundance stratified by frequency category – 'small' (\leq 0.05%), 'medium' (0.05–0.5%), 'large' (0.5–5%), and 'hyperexpanded' (>5%) – is visualized across PV patients ranked by age (x-axis). (C, D) The proportion of 'small' clonotypes within the TRG and TRD repertoires declines significantly with age in PV patients (C), while the proportion of 'hyperexpanded' clonotypes increases (D). These trends are not seen in healthy controls. (E, F) Treemaps comparing age-matched PV patients and healthy controls demonstrate increased clonal dominance in older PV patients within both TCRγ (E) and TCRδ (F) repertoires, relative to controls. (G, H) Cumulative frequency plots of the top 10 most abundant TRG (G) and TRD (H) clonotypes reveal greater clonal skewing in older PV patients (>40 years, N = 6), compared to younger PV patients (<40 years, N = 10) and age-matched healthy controls (N = 3 and N = 12, respectively). For each rank position (1–10), the median cumulative frequency and interquartile range (IQR) across individuals in each group were calculated. Spearman correlation coefficients (R) and corresponding p-values are indicated in panels (A, C, D).



Age- and CMV-associated shifts in TRDV1 and TRGV2 clonotypes in healthy controls and psoriasis patients. (**A, B**) In HC (N = 15), TRDV1(**A**) and TRGV2 (**B**) clonotypes increase with age, whereas in PV patients (N = 26), these clonotype counts decline. (**C**) The proportion of TRDV1 clonotypes within the 'large' (0.5 – 5%) compartment positively correlates with CMV IgG levels in both PV (N = 30) and HC (N = 15). (**D**) The proportion of TRGV2 clonotypes in 'large' compartment is positively correlated with CMV IgG levels in HC, but this relationship is absent in PV patients. Spearman correlation coefficients (R) and p-values are shown for each group. In age-related correlation analyses panels (**A, B**), four oldest PV donors were excluded due to the lack of matched healthy controls.

pattern for TRGV4 (Supplementary Figure 7B), together with elevated D50 values, indicating broader, polyclonal diversification in psoriasis blood. In contrast, skin TCRγ overlap and JI values were similar between PV and HC, with only ten public skin TCRγ clonotypes absent from blood (Supplementary Table 14). Paired blood-skin analysis in eight participants (5 PV, 3 HC) further revealed sharing of γδTCR clonotypes in six participants (4 PV, 2 HC; Figures 7A-B). This involved nine public clonotypes, including five TRGV9-TRGJP rearrangements such as germline-encoded CALWEVQELGKKIKVF, CALWEVRELGKKIKVF, and CALWEVLELGKKIKVF, three TRGV4-TRGJ2 and one TRGV2-TRGJ2 variant (Figures 7C-D). Four of these nine occurred

exclusively in lesional skin. Limited but mostly private TCR δ overlaps were also detected, mainly TRDV2–TRDD3–TRDJ1 rearrangements, including two public clonotypes (CACDVLGDPYTDKLIF and CACDRLGDTDKLIF) that were more frequent in PV blood (16 PV vs. 8 HC and 4 PV vs. 1 HC, respectively). Comparison with the Harden et al. dataset (36), confirmed detection of all nine public blood-skin TCR γ clonotypes in lesional skin, with several absent from healthy skin. Notably, CALWEVRELGKKIKVF, enriched in lesional but not healthy skin, also matched lesional pool from Harden et al., supporting recruitment of circulating V γ 9V δ 2 T cells (23) to inflamed tissue.Together, these findings point to systemic

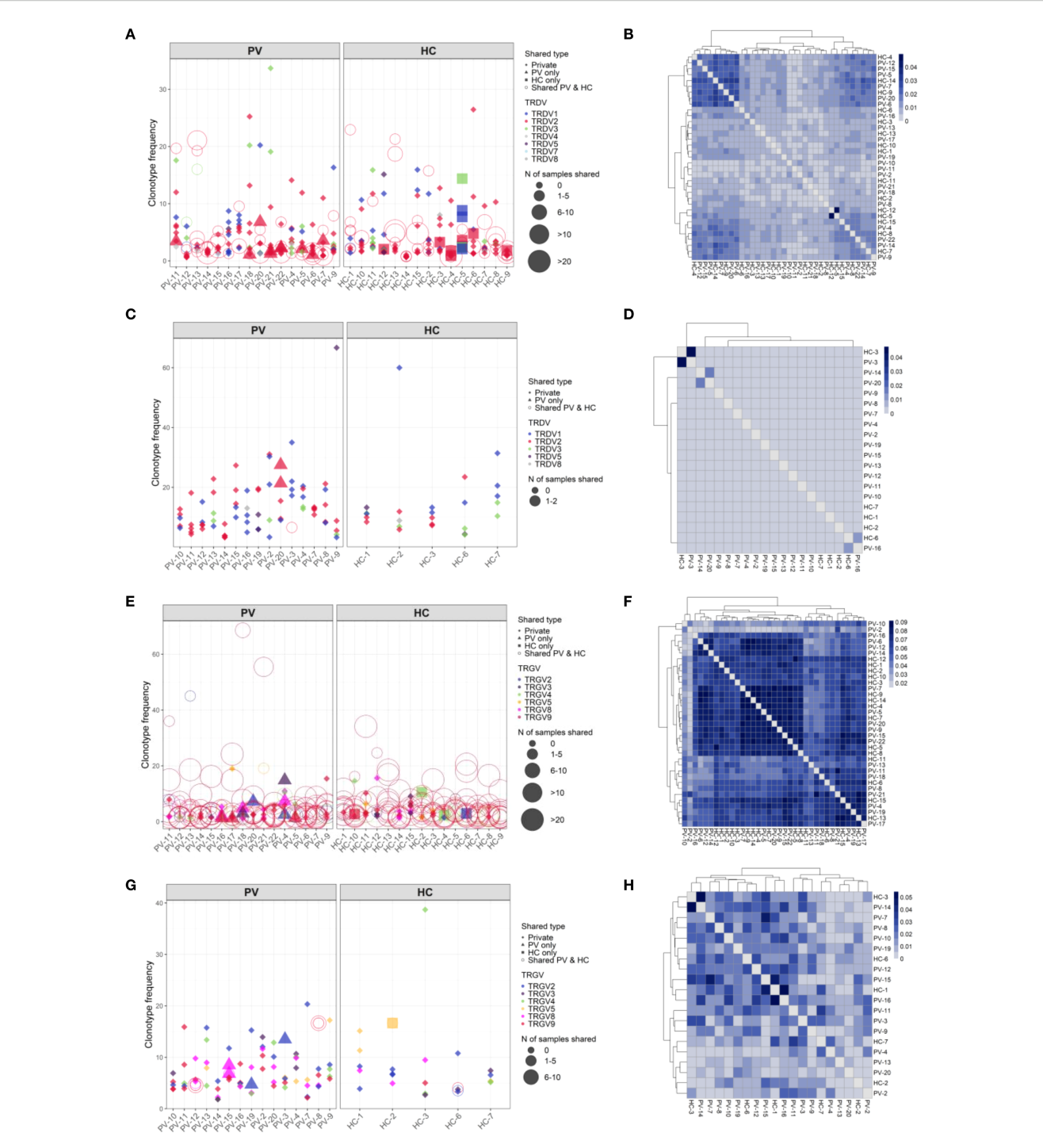
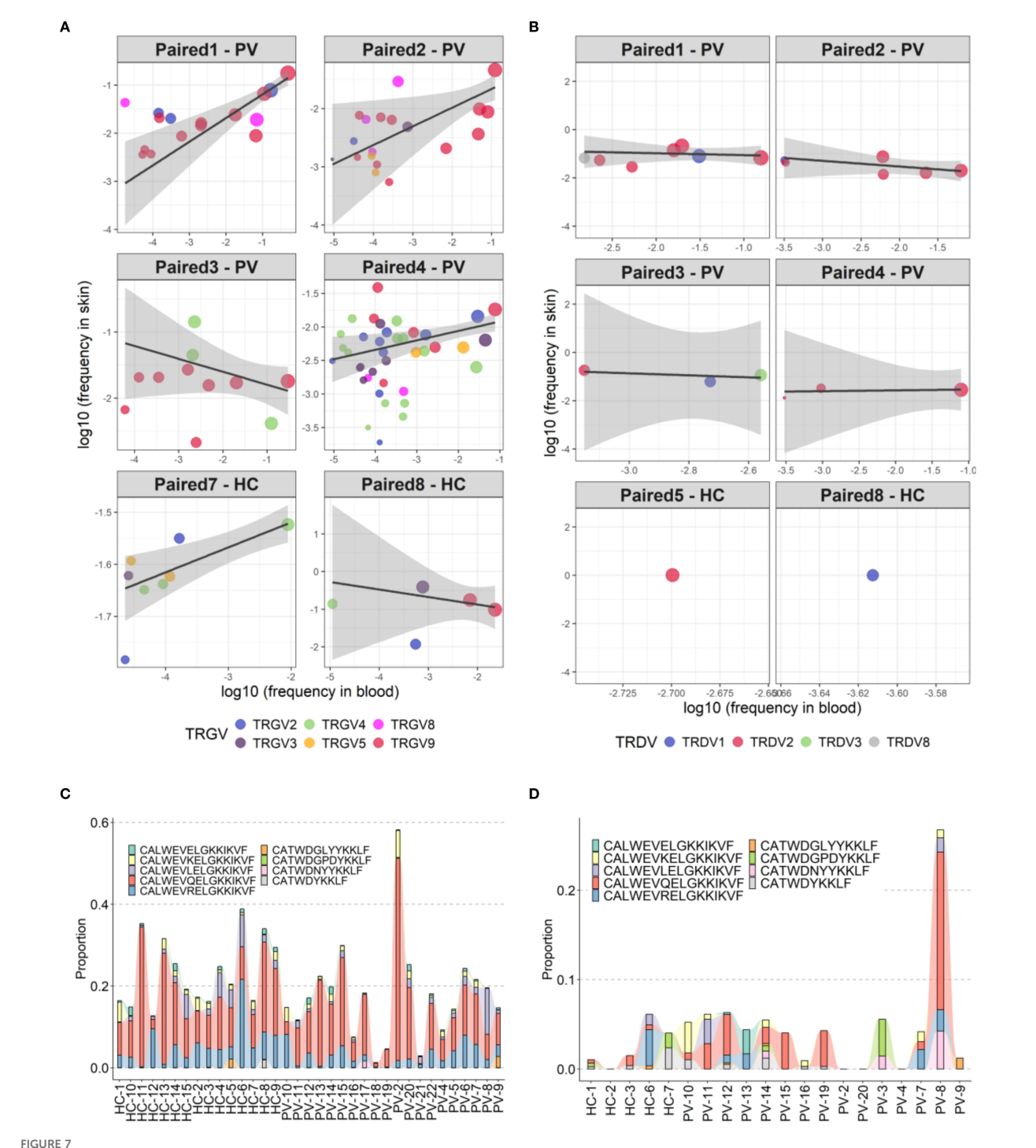


FIGURE 6

TCR δ clonotypes are predominantly private in both blood and skin, whereas TCR γ repertoires display greater inter-individual sharing. Frequencies of the top TCR δ and TCR γ clonotypes in peripheral blood and skin of psoriasis vulgaris (PV) patients and healthy controls (HC). Top 10 clonotypes are shown unless fewer were detected; in skin samples with low TCR δ clonotype counts, the top 5 are shown. Each point represents a unique clonotype; symbol size indicates the number of individuals sharing that clonotype, and color denotes the V gene segment used. TCR δ clonotypes are largely private in both blood (A) and skin (C). In contrast, TCR γ repertoires demonstrate higher public sharing particularly in blood (E), while skinderived TRG clonotypes (G) are more private but still more commonly shared than their δ -chain counterparts. (B, D, F, H) Pairwise Jaccard similarity matrices show the extent of inter-individual clonotype overlap. TCR δ repertoires in blood (B) and skin (D) display low similarity between individuals, whereas TCR γ repertoires exhibit higher overlap in blood (F) and moderate overlap in skin (H), consistent with greater public repertoire characteristics.



Partial overlap of circulating and skin-resident TCR $\gamma\delta$ clonotypes in psoriasis and healthy controls. (**A**, **B**) Clonotype sharing between peripheral blood and lesional skin for TCR γ (**A**) and TCR δ (**B**) repertoires in six individuals. Each point represents a unique clonotype; point size reflects the mean frequency across compartments (log-transformed), and color indicates the TRGV gene segment. Trend lines depict weighted linear models, emphasizing relative distribution without formal regression statistics, which were omitted due to low clonotype counts in some samples. (**C**, **D**) Frequency distribution of nine public TCR γ clonotypes shared across peripheral and skin-resident $\gamma\delta$ T cells in psoriasis patients and healthy controls, shown separately for peripheral blood (**C**) and skin (**D**).

polyclonal $\gamma\delta$ diversification in psoriasis with stable cutaneous repertoires and partial blood–skin sharing of public clonotypes consistent with infiltration of circulating $\gamma\delta T$ cells.

3.7 Transcriptional rewiring of circulating $\gamma\delta$ T cells in psoriasis reveals a hyperactivated, cytotoxic, tissue-homing effector state

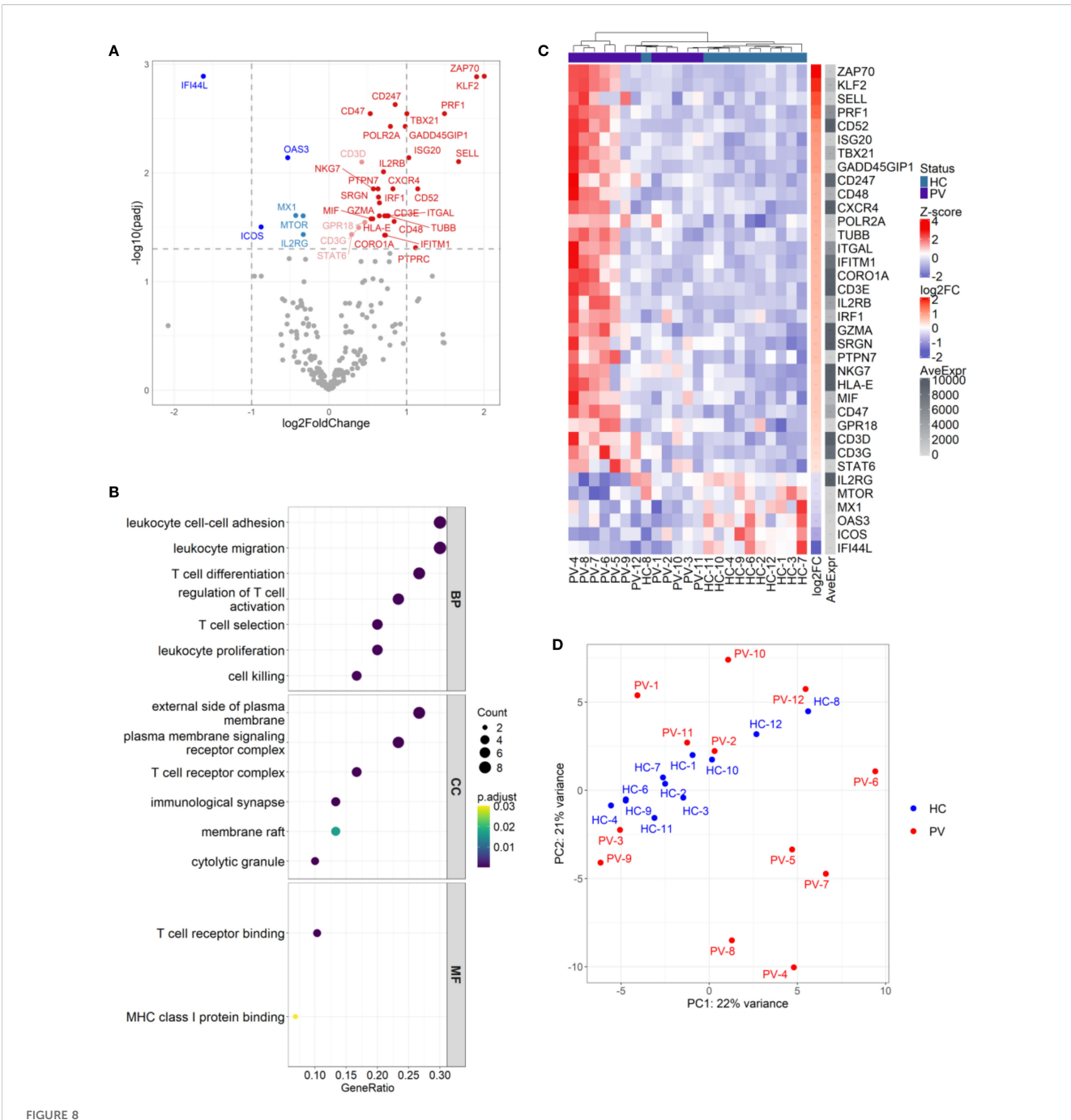
To probe the functional alterations of circulating $\gamma\delta$ T cells in psoriasis, we analyzed gene expression of 395 immunologically relevant genes in FACS-sorted cells from 24 participants (12 PV, 12 HC). Differential expression analysis revealed 36 genes with altered expression (30 upregulated, 6 downregulated), describing a transcriptional profile that positions circulating $\gamma\delta$ T cells as active participants in the inflammatory milieu of psoriasis (Figure 8A, Supplementary Table 15).

Gene ontology and pathway enrichment analysis highlighted coordinated upregulation of processes orchestrating T cell activation, selection, differentiation, adhesion, migration, and cytotoxic function, particularly at immune signaling sites like the TCR complex, immunological synapse, and cytolytic granules (Figure 8B). Consistent with heightened activation, TCR signaling components (CD3D/E/G, CD247, and ZAP70) and the costimulatory CD48 (41) were upregulated, with enrichment in the KEGG "T cell receptor signaling pathway" (adj. p value: 6.34 x 10⁻⁴) and the Biocarta TCR pathway (adj. p value: 4.93 x 10⁻⁶; Supplementary Figure 8). A robust type-1 effector phenotype was supported by upregulation of TBX21 and IRF1, IFN-γ-inducible genes (IFITM1, ISG20) and the stress-responsive, IFN-γ promoting gene GADD45G (42). Elevated IL2RB, implied increased sensitivity to IL-2 and IL-15 cytokines that potentiate γδ T cell cytotoxicity by inducing perforin, T-bet, and Emes transcription (43). Correspondingly, cytotoxic mediators such as PRF1, GZMA, SRGN, and NKG7 were upregulated, paralleling signatures seen in αβ T cells in psoriasis (44–46). Enrichment of the KEGG "Natural killer cell mediated cytotoxicity" pathway (Gene ratio: 6/20, adjusted p value: 2.53 x 10-4) and the Biocarta cytotoxic T lymphocyte (CTL) pathway (Gene ratio: 6/14, adjusted p value: 8.3 x 10⁻⁹) (Supplementary Figure 8 and Supplementary Figure 9) further supported this cytotoxic imprint. Upregulation of KLF2, SELL, and ITGAL indicated increased trafficking capacity (47, 48), while elevated CXCR4 expression suggested directed migration to skin, consistent with reports of CXCR4 upregulation in psoriatic lesions (44, 49), and dermal γδ T cells (6). Expression of CD47 and HLA-E implied immune evasion potential, via resistance to phagocytosis (50) and engagement with inhibitory NK receptors (CD94/NKG2A) (51). In contrast, antiviral genes MX1, OAS3, and IFI44L were suppressed in γδ T cells in psoriasis, suggesting that these cells may be less primed to combat viral threats; alternatively, this finding could reflect an upregulation of these genes within the control group. Importantly, peripheral $\gamma\delta$ T cell subset proportions (V δ 1, V δ 2, V δ 1 V δ 2 did not differ between groups (Supplementary Table 16), confirming these transcriptional shifts were not due to compositional bias. Adding a further layer of complexity, principal component analysis (PCA) revealed a heterogeneity in the upregulated gene signature across psoriasis patients, with a subset of individuals (PV-A: PV-4, PV-5, PV-6, PV-7, PV-8, and PV-9) clustering apart from both controls and other PV patients (termed PV-B), who interspersed with healthy controls (Figures 8C, D). Comparing gene expression between different subsets (PV-A vs. HC, PV-B vs. HC, and PV-A vs. PV-B) showed that the psoriasis-associated γδ T cell signature was largely driven by the PV-A subgroup. In the PV-A vs. HC comparison, all previously identified upregulated genes remained, along with additional elevated, as well as downregulated transcripts (Supplementary Figure 10). Of note, the statistical significance of certain genes, such as ZAP70, was markedly enhanced (adjusted p-value dropped from 0.001 to 3.78 x10⁻²³, and log₂fold increased from 2 to 3.01). In contrast, the PV-B vs. HC comparison revealed no significant DEGs, supporting the idea that PV-B patients have a transcriptional profile akin to healthy individuals. However, while many of the upregulated genes in the PV-A vs. HC analysis were also present in the PV-A vs. PV-B comparison, several transcripts (SELL, CD247, POLR2A, SRGN, NKG7, CD3D, CD3G, and STAT6) were not differentially expressed in the PV-A vs. PV-B comparison, provoking the thought that two subgroups represent different levels along a continuum of immune activation, with PV-A likely reflecting a more robust activation, and PV-B indicating a subtler, intermediate level of response. Interestingly, this heterogeneity could not be explained by age, PASI score, disease duration, sex, CMV status, and γδ T cell subset proportions, leaving the underlying drivers of this variability unresolved. This divergence may reflect distinct disease endotypes, differences in immune microenvironments, or other yet unidentified factors shaping $\gamma\delta$ T cell function in psoriasis.

4 Discussion

Psoriasis vulgaris (PV) is a chronic inflammatory dermatosis where prominent role has been assigned to T cells. Most prior studies in humans and mice, have focused on $\alpha\beta$ T cells, leaving the roles of $\gamma\delta$ T lymphocytes relatively understudied. In this study, we combined flow cytometry, mRNA profiling and TCR sequencing for integrated analysis of circulating and cutaneous $\gamma\delta$ T cells of PV patients and healthy controls, correlating these data with clinical, demographic, and anthropometric features. We found that psoriasis induces distinct and tissue-specific remodeling of the $\gamma\delta$ T cell compartment, including alterations in cell frequency, gene expression, and TCR repertoire architecture. These changes were shaped by a complex interplay of sex, age, disease severity and chronicity, and differed between blood and lesional skin of PV patients.

Consistent with previous studies (6, 52–54), psoriatic lesions were enriched for CD3⁺ T cells, while total $\gamma\delta$ T cell frequencies remained comparable to healthy skin. Nonetheless, TRG/TRD transcripts positively correlated with disease severity and duration, suggesting increased transcriptional activity or clonal



Circulating $\gamma\delta$ T cells in psoriasis patients display differential effector gene signatures with inter-individual heterogeneity. (A) Differential expression analysis of 300 genes in $\gamma\delta$ T cells from psoriasis patients (N = 12) versus healthy controls (N = 11) revealed 36 significantly modulated genes (30 upregulated, 6 downregulated; adj.p < 0.05). Color coding reflects significance and fold change: dark red/blue for $\log_2 FC > \pm 1$, light red/blue for $\log_2 FC < \pm 1$; non-significant genes are grey. (B) Gene ontology (GO) enrichment analysis of upregulated genes identified pathways involved in T cell activation, adhesion, migration, and cytotoxicity. Dot size represents gene ratio; color indicates adjusted p-value. GO terms are grouped by BP (Biological Process), CC (Cellular Component), and MF (Molecular Function). (C) Heatmap of differentially expressed genes (rows) across individual samples (columns), with Z-score normalization. Samples are hierarchically clustered, and group identity is indicated by a color bar. (D) Principal component analysis (PCA) plot shows partial segregation of a subset of psoriasis samples (PV-4 to PV-9) from other patients and controls, indicating inter-individual transcriptional heterogeneity.

skewing rather than true cellular expansion. An age-associated decline in cutaneous $\gamma\delta$ T cells was observed in psoriasis but not in healthy skin, suggesting that chronic inflammation perturbs local $\gamma\delta$ T cell homeostasis typically maintained during physiological ageing (55). Contrary to earlier reports of V γ 9V δ 2 enrichment in

psoriatic lesions (8, 19), we observed no expansion of the V δ 2⁺ compartment. Because our panel lacked V γ 9-chain staining, the V δ 2⁺ population likely included non-V γ 9 tissue-resident cells (23, 56), preventing direct assessment of V γ 9V δ 2 dynamics and potentially masking previously reported subset-specific alterations

(8, 19). Instead, we observed enrichment of $V\delta 1^{-}V\delta 2^{-}$ subset in lesional skin, hinting at expansion of unconventional or tissueadapted subsets. Interestingly, skin $V\delta2^+$ frequencies increased with higher PASI scores in female patients only, suggesting potential sexspecific contribution to PV immunopathology. This sex-specific pattern extended to the peripheral blood, where male patients showed reduced $V\delta2^+$ cells, consistent with prior reports (8, 19), though not previously associated with sex. Whether this pattern reflects true biological variation or is influenced by cohort composition remains to be clarified. Of note, healthy female controls in our cohort displayed lower baseline $\gamma\delta$ and $V\delta2^+$ frequencies than males, contrasting prior reports (30, 31), which may have attenuated case-control differences in our unstratified analyses. Importantly, Laggner et al. demonstrated that circulating Vγ9Vδ2 reductions were largely restricted to the skin-homing CLA⁺ subset (8) which we did not assess, potentially explaining differences between our findings and previous reports. In addition to numerical differences, female patients displayed a higher prevalence of longer TRDV2-TRDJ3 rearrangements, diverging from the canonical TRDV2-TRDJ1 usage typically seen in healthy individuals (23). These structural differences were absent in healthy male and female controls, implicating psoriasis as the primary driver of this repertoire divergence. Longer TRDV2-TRDJ3 rearrangements have been previously associated with extrathymic maturation of fetal $\gamma\delta$ T cells (57), but their role or origin in the peripheral repertoire of adult female psoriasis patients remains unclear. However, given the male-biased composition of our cohort, these observations warrant validation in larger, sex-balanced populations to clarify their relevance to disease pathogenesis.

In addition to sex-associated differences, psoriasis was associated with marked structural changes of peripheral and cutaneous γδTCR repertoires. As an initial observation, both healthy and lesional skin exhibited shorter TRG CDR3 regions compared to blood, largely due to alternative TRGV-J gene pairing. This was accompanied by a bimodal distribution of TRGV9 CDR3 lengths, driven by increased usage of TRGV9-TRGJ2 combinations, and distinct TRD CDR3 length profiles between blood and skin. In blood, TRDV2 distributions were predominantly Gaussian-like, while TRDV1 and TRDV3 exhibited bimodal profiles. In contrast, the skin repertoire showed a more balanced TRDV1/TRDV2 representation with a bimodal and elongated TRDV2 landscape, and only a few dominant TRDV1 and TRDV3 peaks, suggesting selective pressures and receptor skewing in the cutaneous microenvironment. Psoriasis-specific repertoire remodeling was apparent beyond these tissue-specific features. Psoriasis severity correlated with increased CDR3 length and junctional diversity, particularly within TRGV8 and TRDV2 clonotypes. Additionally, longer TRDV1/2/3 rearrangements were largely absent in healthy skin, supporting a model in which inflammatory signaling in lesional tissue drives enhanced receptor remodeling and clonal diversification - consistent with findings in rheumatoid arthritis, where longer TRD rearrangements were similarly enriched (58). These structural shifts mirror those described in peripheral $\gamma\delta$ T cells upon aging (32, 59). Specifically, naive subsets in young adults typically exhibit Gaussian-like TRD CDR3 distributions, whereas central memory (T_{CM} CD27⁺CD45RA⁻) and effector memory (T_{EM} CD27 CD45RA subsets gradually adopt more skewed distributions, and terminally differentiated effector memory cells (T_{EMRA} CD27⁻CD45RA⁺) display dominant peaks and reduced diversity. Supporting this interpretation, Vγ9Vδ2 cells in psoriasis patients have previously been shown to adopt a CD27 CD45RA+ terminal phenotype, accompanied by contraction of the central memory pool (19). Whether similar subset redistribution occurs within lesional skin, and whether this contributes to the distinct repertoire features we identified here, remains to be clarified in future studies. The most striking hallmark of psoriasis-associated γδTCR dysregulation was a marked attrition of peripheral repertoire diversity coupled with selective depletion of clonotypes in the skin. Although total clonotype counts were comparable between groups, higher PASI scores were associated with lower repertoire diversity, loss of rare clonotypes, and expansion of dominant clones, particularly within the TRGV9 and TRDV2 subsets. This loss of peripheral diversity was consistent across multiple analytical metrics and coincided with depletion of hyperexpanded TRGV8 clones in lesional skin. At the same time, medium-sized TRGV4 clonotypes became increasingly represented in both blood and skin, suggesting targeted remodeling of circulating and tissue-resident $\gamma\delta$ subsets in PV. A particularly notable finding was the loss of shared/public TRGV8, and to a lesser extent, TRGV4 clonotypes in PV blood, indicating increasing peripheral repertoire heterogeneity. This divergence was, moreover, associated with elevated TRGV8 and TRGV4 D50 values in the blood of psoriasis patients, consistent with polyclonal expansion and diversification rather than dominance of few expanded clones. These features parallel findings in $\gamma\delta$ and $\alpha\beta$ T cells in autoimmune (58) and chronic inflammatory conditions (60), where persistent antigenic stimulation drives personalised, heterogeneous immune responses. By contrast, healthy individuals showed more conserved, public TRGV4 and TRGV8 repertoires, consistent with CMVassociated clonal expansions of Vy8 and Vy4 TCRs (61), highlighting the disease-specific nature of the repertoire changes observed in PV.

Beyond disease severity, aging also emerged as a dominant, independent driver of the peripheral γδTCR repertoire contraction, often exceeding the effects of disease severity. In blood of PV patients, increasing age correlated with a progressive loss of small and medium-sized clonotypes, particularly within TRGV9 and TRDV2 subsets, along with compensatory rise in hyperexpanded clones, suggestive of repertoire contraction and skewing. While healthy individuals displayed age-related expansions in TRGV2 and TRDV1 clonotypes, likely linked to CMV seropositivity (26, 35, 62-64), in PV, CMV further intensified TRDV2 depletion and TRDV1 expansion. However, as CMV titers did not correlate with age or disease severity in PV, CMV alone could not fully account for the age and disease-related repertoire changes. Importantly, this collapse in peripheral TRDV2 repertoire in PV occurred independently of changes in Vδ2⁺ cell frequencies, pointing to true repertoire contraction rather than a reduction in circulating cell numbers. Aging was also associated with higher cumulative frequencies of dominant clones and elongation of CDR3δ regions,

primarily due to increased NDN insertions, particularly in non-TRDV2 rearrangements. These age-associated patterns resemble repertoire changes described in both $\gamma\delta$ (65) and $\alpha\beta$ T cells (66, 67) of older individuals, where longer CDR3 regions contribute to enhanced cross-reactivity and reduced TCR specificity (68). The observed contraction in TRGV9 and TRDV2 repertoires with increasing age and disease severity resembles the features of "latestage differentiated" CD27 CD28 CD16 Vγ9Vδ2 cells (69). Specifically, CD27 Vγ9Vδ2 T subsets show significantly fewer clonotypes and lower diversity in their TCRδ repertoires compared to their CD27⁺ (CD27⁺CD28⁺) counterparts (23, 69), suggesting that more severe or long-standing disease may be associated with a skewing toward cytotoxic, effector-like γδ T cells. Supporting this phenotypic transition, transcriptomic profiling of circulating $\gamma\delta$ T cells in our cohort revealed a strongly pro-inflammatory and cytotoxic signature, marked by elevated TCR signaling (CD3D/E/G, ZAP70, CD247), cytotoxic effectors (PRF1, GZMA, NKG7, SRGN), Th1 polarization (IL2RB, TBX21, IRF1, GADD45G), and tissue-homing markers (CXCR4, KLF2). These transcriptional features are consistent with functionally primed cells capable of migrating to inflamed tissue (47, 70, 71) and contributing to psoriatic pathology (43, 46, 49, 72). Notably, they overlap with the transcriptional profiles of NK and CD8⁺ $T_{EM}/T_{TEMRA} \alpha\beta T$ cells in psoriasis (44-46, 72), positioning γδ T cells as integral components of the effector immune response in this disease. However, substantial inter-individual variability was observed, with some patients showing transcriptional profiles similar to healthy controls. These findings align with prior reports of cellular and molecular heterogeneity in psoriasis (72-74) and imply the existence of distinct disease endotypes that may vary with severity and duration, arguing in favor of a longitudinal studies integrating single-cell data to uncover these dynamics and their clinical implications.

Several public TRGV9-TRGJP clonotypes, including germlineencoded variants, were consistently observed in blood and lesional skin and also detected in external psoriasis datasets (36), indicating their potential recurrence in inflamed tissues. However, their frequent presence in healthy individuals, as shown for CALWEVQELGKKIKVF and CALWEVRELGKKIKVF, in both our data and prior studies (23, 36, 75), suggests that they are widely distributed, skin-homing variants with limited association to psoriasis. Aside from these ubiquitously shared variants, most clonotypes remained private, particularly in the skin-derived TCRδ repertoires, while TCRγ clonotypes were more commonly shared across individuals and compartments. Nonetheless, nearly half of all skin-derived TCRy (41.07%) and a smaller fraction of TCRδ (17.42%) clonotypes were also present in blood, similarly distributed between PV and controls, indicating that cutaneous $\gamma\delta$ T cells may derive from circulating pools in both health and disease. Of interest, few public clonotypes appeared restricted to either PV or healthy blood samples, but none showed statistically significant enrichment after correction. Similarly, skin-specific clonotypes, such as CALWEVKELGKKIKVF in PV lesional skin, showed intriguing but statistically inconclusive patterns. Several public lesional skin clonotypes also overlapped with those reported by

Harden et al. (36), further hinting at possible disease relevance. However, the lack of statistical significance and the small sample size preclude firm conclusions regarding their functional roles or diagnostic utility. Future application of single-cell TCR sequencing could allow unambiguous linking of γ - and δ -chains within individual cells and greatly improve the interpretability of our repertoire data.

In summary, psoriasis drives compartment-specific, inflammation-associated changes of the γδTCR repertoire, marked by peripheral contraction, cutaneous reshaping, and structural instability influenced by age, disease, and sex. A central novelty of our study is the comprehensive characterisation of the diversity and frequency of multiple γδ T cell subsets, including, but not limited to, Vγ9Vδ2 in both blood and healthy/lesional skin. By capturing a broader fraction of the γδ-cell pool, our work extends current understanding and may ultimately facilitate the development of more accessible algorithms for routine monitoring of disease activity. Although robust evidence for public disease-specific clonotypes remain elusive, gene expression profiling identifies a functionally active, tissue-homing subset of $\gamma\delta$ T cells likely to contribute to pathogenesis in a patient-specific manner. Collectively, these findings advance our understanding of PV by linking repertoire architecture and functional states to disease heterogeneity, providing a framework for stratifying patients based on immune profiles. Furthermore, γδ T cells emerge as promising targets for therapeutic intervention, either by modulating their recruitment, effector functions, or clonal composition. Future studies employing larger, sex-balanced cohorts, single-cell TCR/RNA sequencing, and longitudinal sampling are warranted to refine these observations and translate them into clinical strategies.

Data availability statement

The RNA-seq and TCR-seq datasets from peripheral blood samples can be found in the NCBI SRA, under the BioProjects PRJNA1293314 (https://www.ncbi.nlm.nih.gov/sra/PRJNA1293314) and PRJNA1292788 (https://www.ncbi.nlm.nih.gov/sra/PRJNA1292788), respectively. TCR-seq data from skin samples will be made available under BioProject PRJNA1293805 upon publication of forthcoming analysis focused on $\alpha\beta$ TCR repertoires.

Ethics statement

The studies involving humans were approved by Ethics Committee of the Faculty of Medicine in Osijek (Certificate No. 2158-61-07-19-126, October 11, 2019). Ethics Committee of the Clinical Hospital Centre Osijek (Certificate No. R2-12487/2019, September 12, 2019). The studies were conducted in accordance with the local legislation and institutional requirements. The participants provided their written informed consent to participate in this study.

Author contributions

MJ: Data curation, Formal analysis, Investigation, Methodology, Visualization, Writing – original draft, Writing – review & editing. MMi: Investigation, Methodology, Resources, Writing – review & editing. MSa: Conceptualization, Validation, Writing – review & editing. VP: Data curation, Investigation, Resources, Writing – review & editing. MŠo: Investigation, Resources, Writing – review & editing. MT-L: Resources, Writing – review & editing. MMa: Investigation, Writing – review & editing. PB: Writing – review & editing. ST: Conceptualization, Funding acquisition, Investigation, Methodology, Project administration, Supervision, Validation, Writing – original draft, Writing – review & editing.

Funding

The author(s) declare financial support was received for the research and/or publication of this article. This research was funded by the Intramural Research Programme of the Josip Juraj Strossmayer University (grant number IP6-2021-MEFOS, IP10-2024-MEFOS, IP23-2025-MEFOS) and the Croatian Science Foundation project "NGS analysis of MAIT and $\gamma \delta T$ cell transcriptome: phenotype, function and TCR repertoire in the etiology of Psoriasis Vulgaris" (UIP-2019-04-3494). Research at the Department of Immunology and Biotechnology, University of Pécs was supported by TKP-2021-EGA-10 funding.

Acknowledgments

The authors thank Ms. Noémi Balázs for performing FACS sorting using Bio-Rad S3e sorter at the Department of Immunology and Biotechnology, and Dr. Dávid Ernszt for their kind support with flow cytometry using the FACS Canto II at the Szentágothai János Research Center, University of Pécs, Hungary.

References

- 1. Hawkes JE, Chan TC, Krueger JG. Psoriasis pathogenesis and the development of novel, targeted immune therapies. *J Allergy Clin Immunol.* (2017) 140:645–53. doi: 10.1016/j.jaci.2017.07.004
- 2. Matos TR, O'Malley JT, Lowry EL, Hamm D, Kirsch IR, Robins HS, et al. Clinically resolved psoriatic lesions contain psoriasis-specific IL-17–producing $\alpha\beta$ T cell clones. J Clin Invest. (2017) 127:4031–41. doi: 10.1172/JCI93396
- 3. Ortega C, Fernández- AS, Carrillo JM, Romero P, Molina IJ, Moreno JC, et al. IL-17-producing CD8+ T lymphocytes from psoriasis skin plaques are cytotoxic effector cells that secrete Th17-related cytokines. *J Leukocyte Biol.* (2009) 86:435-43. doi: 10.1189/JLB.0109046
- 4. Res PCM, Piskin G, de Boer OJ, van der Loos CM, Teeling P, Bos JD, et al. Overrepresentation of IL-17A and IL-22 producing CD8 T cells in lesional skin suggests their involvement in the pathogenesis of psoriasis. *PloS One.* (2010) 5(11): e14108. doi: 10.1371/journal.pone.0014108
- 5. Liu J, Chang H-W, Huang Z-M, Nakamura M, Sekhon S, Ahn R, et al. Single-cell RNA sequencing of psoriatic skin identifies pathogenic Tc17 cell subsets and reveals distinctions between CD8+ T cells in autoimmunity and cancer. *J Allergy Clin Immunol.* (2021) 147:2370–80. doi: 10.1016/j.jaci.2020.11.028
- 6. Cai Y, Shen X, Ding C, Qi C, Li K, Li X, et al. Pivotal role of dermal IL-17-producing $\gamma\delta$ T cells in skin inflammation. *Immunity*. (2011) 35:596–610. doi: 10.1016/j.immuni.2011.08.001

Conflict of interest

The authors declare that the research was conducted in the absence of any commercial or financial relationships that could be construed as a potential conflict of interest.

Generative Al statement

The author(s) declare that no Generative AI was used in the creation of this manuscript.

Any alternative text (alt text) provided alongside figures in this article has been generated by Frontiers with the support of artificial intelligence and reasonable efforts have been made to ensure accuracy, including review by the authors wherever possible. If you identify any issues, please contact us.

Publisher's note

All claims expressed in this article are solely those of the authors and do not necessarily represent those of their affiliated organizations, or those of the publisher, the editors and the reviewers. Any product that may be evaluated in this article, or claim that may be made by its manufacturer, is not guaranteed or endorsed by the publisher.

Supplementary material

The Supplementary Material for this article can be found online at: https://www.frontiersin.org/articles/10.3389/fimmu.2025.1670364/full#supplementary-material

- 7. Pantelyushin S, Haak S, Ingold B, Kulig P, Heppner FL, Navarini AA, et al. Rorythinnate lymphocytes and $\gamma\delta$ T cells initiate psoriasiform plaque formation in mice. *J Clin Invest.* (2012) 122:2252–6. doi: 10.1172/JCI61862
- 8. Laggner U, Di Meglio P, Perera GK, Hundhausen C, Lacy KE, Ali N, et al. Identification of a novel proinflammatory human skin-homing $V\gamma9V\delta2$ T cell subset with a potential role in psoriasis. *JI*. (2011) 187:2783–93. doi: 10.4049/jimmunol.1100804
- 9. Plužarić V, Štefanić M, Mihalj M, Tolušić Levak M, Muršić I, Glavaš-Obrovac I, et al. Differential skewing of circulating MR1-restricted and $\gamma\delta$ T cells in human psoriasis vulgaris. Front Immunol. (2020) 11:572924. doi: 10.3389/fimmu.2020.572924
- 10. Tokić S, Jirouš M, Plužarić V, Mihalj M, Šola M, Tolušić Levak M, et al. The miR-20a/miR-92b profile is associated with circulating γδ T-cell perturbations in mild psoriasis. *Int J Mol Sci.* (2023) 24:4323. doi: 10.3390/ijms24054323
- 11. Hartwig T, Pantelyushin S, Croxford AL, Kulig P, Becher B. Dermal IL-17-producing $\gamma\delta$ T cells establish long-lived memory in the skin. *Eur J Immunol.* (2015) 45:3022–33. doi: 10.1002/eji.201545883
- 12. Roark CL, Huang Y, Jin N, Aydintug MK, Casper T, Sun D, et al. A canonical V γ 4V δ 4+ γ δ T cell population with distinct stimulation requirements which promotes the Th17 response. *Immunol Res.* (2013) 55:217–30. doi: 10.1007/s12026-012-8364-9
- 13. Sumaria N, Roediger B, Ng LG, Qin J, Pinto R, Cavanagh LL, et al. Cutaneous immunosurveillance by self-renewing dermal gammadelta T cells. *J Exp Med.* (2011) 208:505–18. doi: 10.1084/jem.20101824

- 14. Kelsen J, Dige A, Christensen M, D'Amore F, Iversen L. Frequency and clonality of peripheral $\gamma\delta$ T cells in psoriasis patients receiving anti-tumour necrosis factor- α therapy: Gamma-delta T cells in psoriasis patients. Clin Exp Immunol. (2014) 177:142–8. doi: 10.1111/cei.12331
- 15. van der Fits L, Mourits S, Voerman JSA, Kant M, Boon L, Laman JD, et al. Imiquimod-induced psoriasis-like skin inflammation in mice is mediated via the IL-23/IL-17 axis. *J Immunol*. (2009) 182:5836–45. doi: 10.4049/jimmunol.0802999
- 16. Gatzka M, Hainzl A, Peters T, Singh K, Tasdogan A, Wlaschek M, et al. Reduction of CD18 promotes expansion of inflammatory $\gamma\delta$ T cells collaborating with CD4 $^+$ T cells in chronic murine psoriasiform dermatitis. *JI*. (2013) 191:5477–88. doi: 10.4049/jimmunol.1300976
- 17. Ramírez-Valle F, Gray EE, Cyster JG. Inflammation induces dermal $V\gamma 4^+\gamma \delta T17$ memory-like cells that travel to distant skin and accelerate secondary IL-17–driven responses. *Proc Natl Acad Sci USA*. (2015) 112:8046–51. doi: 10.1073/pnas.1508990112
- 18. Nakamizo S, Egawa G, Tomura M, Sakai S, Tsuchiya S, Kitoh A, et al. Dermal V γ 4 + γ 8 T cells possess a migratory potency to the draining lymph nodes and modulate CD8 + T-cell activity through TNF- α Production. *J Invest Dermatol.* (2015) 135:1007–15. doi: 10.1038/jid.2014.516
- 19. Zhou J, Zhang J, Tao L, Peng K, Zhang Q, Yan K, et al. Up-regulation of BTN3A1 on CD14+ cells promotes $V\gamma9V\delta2$ T cell activation in psoriasis. *Proc Natl Acad Sci.* (2022) 119:e2117523119. doi: 10.1073/pnas.2117523119
- 20. Chen Y, Fu Q, Ma Y, Wang N, Yang J, Liang Q, et al. Identification of the immune repertoire of $\gamma\delta$ T-cell receptors in psoriasis. *Immunol Cell Biol.* (2024) 102:570–7. doi: 10.1111/imcb.12765
- 21. Gray JI, Caron DP, Wells SB, Guyer R, Szabo P, Rainbow D, et al. Human $\gamma\delta$ T cells in diverse tissues exhibit site-specific maturation dynamics across the life span. Sci Immunol. (2024) 9:eadn3954. doi: 10.1126/sciimmunol.adn3954
- 22. Hunter S, Willcox CR, Davey MS, Kasatskaya SA, Jeffery HC, Chudakov DM, et al. Human liver infiltrating $\gamma\delta$ T cells are composed of clonally expanded circulating and tissue-resident populations. *J Hepatol.* (2018) 69:654–65. doi: 10.1016/j.jhep.2018.05.007
- 23. Davey MS, Willcox CR, Hunter S, Kasatskaya SA, Remmerswaal EBM, Salim M, et al. The human V δ 2+ T-cell compartment comprises distinct innate-like V γ 9+ and adaptive V γ 9- subsets. *Nat Commun.* (2018) 9:1760. doi: 10.1038/s41467-018-04076-0
- 24. Sandstrom A, Peigné C-M, Léger A, Crooks JE, Konczak F, Gesnel M-C, et al. The intracellular B30.2 domain of butyrophilin 3A1 binds phosphoantigens to mediate activation of human $V\gamma9V\delta2$ T cells. *Immunity*. (2014) 40:490–500. doi: 10.1016/j.immuni.2014.03.003
- 25. Rhodes DA, Chen H-C, Price AJ, Keeble AH, Davey MS, James LC, et al. Activation of human $\gamma\delta$ T cells by cytosolic interactions of BTN3A1 with soluble phosphoantigens and the cytoskeletal adaptor periplakin. *J Immunol.* (2015) 194:2390–8. doi: 10.4049/jimmunol.1401064
- 26. Davey MS, Willcox CR, Joyce SP, Ladell K, Kasatskaya SA, McLaren JE, et al. Clonal selection in the human V δ 1 T cell repertoire indicates $\gamma\delta$ TCR-dependent adaptive immune surveillance. *Nat Commun.* (2017) 8:14760. doi: 10.1038/ncomms14760
- 27. Ravens S, Schultze-Florey C, Raha S, Sandrock I, Drenker M, Oberdörfer L, et al. Human $\gamma\delta$ T cells are quickly reconstituted after stem-cell transplantation and show adaptive clonal expansion in response to viral infection. *Nat Immunol.* (2017) 18:393–401. doi: 10.1038/ni.3686
- 28. McMurray JL, von BA, TE T, Syrimi E, GS T, Sharif M, et al. Transcriptional profiling of human V δ 1 T cells reveals a pathogen-driven adaptive differentiation program. *Cell Rep.* (2022) 39(8):110858. doi: 10.1016/j.celrep.2022.110858
- 29. Pizzolato G, Kaminski H, Tosolini M, Franchini D-M, Pont F, Martins F, et al. Single-cell RNA sequencing unveils the shared and the distinct cytotoxic hallmarks of human TCRV δ 1 and TCRV δ 2 $\gamma\delta$ T lymphocytes. . *Proc Natl Acad Sci USA*. (2019) 116 (24):11906-15. doi: 10.1073/pnas.1818488116
- 30. Caccamo N, Dieli F, Wesch D, Jomaa H, Eberl M. Sex-specific phenotypical and functional differences in peripheral human Vgamma9/Vdelta2 T cells. *J Leukoc Biol.* (2006) 79:663–6. doi: 10.1189/jlb.1105640
- 31. Fonseca S, Pereira V, Lau C, Teixeira MDA, Bini-Antunes M, Lima M. Human peripheral blood gamma delta T cells: report on a series of healthy caucasian portuguese adults and comprehensive review of the literature. *Cells*. (2020) 9(3):729. doi: 10.3390/cells9030729
- 32. Kallemeijn MJ, Kavelaars FG, van der Klift MY, Wolvers-Tettero ILM, Valk PJM, van Dongen JJM, et al. Next-generation sequencing analysis of the human TCR $\gamma\delta$ + T-cell repertoire reveals shifts in V γ and V δ -usage in memory populations upon aging. Front Immunol. (2018) 9:448. doi: 10.3389/fimmu.2018.00448
- 33. Argentati K, Re F, Donnini A, Tucci MG, Franceschi C, Bartozzi B, et al. Numerical and functional alterations of circulating gammadelta T lymphocytes in aged people and centenarians. *J Leukoc Biol.* (2002) 72:65–71. doi: 10.1189/jlb.72.1.65
- 34. Kallemeijn MJ, Boots AMH, van der Klift MY, Brouwer E, Abdulahad WH, Verhaar JAN, et al. Ageing and latent CMV infection impact on maturation, differentiation and exhaustion profiles of T-cell receptor gammadelta T-cells. *Sci Rep.* (2017) 7:5509. doi: 10.1038/s41598-017-05849-1
- 35. Pitard V, Roumanes D, Lafarge X, Couzi L, Garrigue I, Lafon M-E, et al. Long-term expansion of effector/memory V δ 2– $\gamma\delta$ T cells is a specific blood signature of CMV infection. *Blood.* (2008) 112:1317–24. doi: 10.1182/blood-2008-01-136713

- 36. Harden JL, Hamm D, Gulati N, Lowes MA, Krueger JG. Deep sequencing of the T-cell receptor repertoire demonstrates polyclonal T-cell infiltrates in psoriasis. *F1000Res.* (2015) 4:460. doi: 10.12688/f1000research.6756.1
- 37. Bolotin DA, Poslavsky S, Mitrophanov I, Shugay M, Mamedov IZ, Putintseva EV, et al. MiXCR: software for comprehensive adaptive immunity profiling. *Nat Methods*. (2015) 12:380–1. doi: 10.1038/nmeth.3364
- 38. Shugay M, Bagaev DV, Turchaninova MA, Bolotin DA, Britanova OV, Putintseva EV, et al. VDJtools: unifying post-analysis of T cell receptor repertoires. *PloS Comput Biol.* (2015) 11:e1004503. doi: 10.1371/journal.pcbi.1004503
- 39. Bioinformatics analysis of T-cell and B-cell immune repertoires . Available online at: https://immunarch.com/ (Accessed July 10, 2025).
- 40. Vilibic-Cavlek T, Kolaric B, Beader N, Vrtar I, Tabain I, Mlinaric-Galinovic G. Seroepidemiology of cytomegalovirus infections in Croatia. *Wien Klin Wochenschr.* (2017) 129:129–35. doi: 10.1007/s00508-016-1069-7
- 41. McArdel SL, Terhorst C, Sharpe AH. Roles of CD48 in regulating immunity and tolerance. Clin Immunol.~(2016)~164:10-20. doi: 10.1016/j.clim.2016.01.008
- 42. Chi H, Lu B, Takekawa M, Davis RJ, Flavell RA. GADD45 β /GADD45 γ and MEKK4 comprise a genetic pathway mediating STAT4-independent IFN γ production in T cells. *EMBO J.* (2004) 23:1576–86. doi: 10.1038/sj.emboj.7600173
- 43. Ribot JC, Ribeiro ST, Correia DV, Sousa AE, Silva-Santos B. Human $\gamma\delta$ Thymocytes Are Functionally Immature and Differentiate into Cytotoxic Type 1 Effector T Cells upon IL-2/IL-15 Signaling. *J Immunol.* (2014) 192:2237–43. doi: 10.4049/jimmunol.1303119
- 44. Suárez-Fariñas M, Fuentes-Duculan J, Lowes MA, Krueger JG. Resolved psoriasis lesions retain expression of a subset of disease-related genes. *J Invest Dermatol.* (2011) 131:391–400. doi: 10.1038/jid.2010.280
- 45. Prpić L, Strbo N, Sotosek V, Gruber F, Podack ER, Rukavina D. Assessment of perforin expression in peripheral blood lymphocytes in psoriatic patients during exacerbation of disease. *Acta Derm Venereol Suppl (Stockh)*. (2000) 211:14–6. doi: 10.1080/00015550050500059
- 46. Zhang B, Roesner LM, Traidl S, Koeken VACM, Xu C-J, Werfel T, et al. Single-cell profiles reveal distinctive immune response in atopic dermatitis in contrast to psoriasis. *Allergy.* (2023) 78:439–53. doi: 10.1111/all.15486
- 47. Bai A, Hu H, Yeung M, Chen J. Kruppel-like factor 2 controls T cell trafficking by activating L-selectin (CD62L) and sphingosine-1-phosphate receptor 1 transcription. *J Immunol.* (2007) 178:7632–9. doi: 10.4049/jimmunol.178.12.7632
- 48. Guttman-Yassky E, Vugmeyster Y, Lowes MA, Chamian F, Kikuchi T, Kagen M, et al. Blockade of CD11a by efalizumab in psoriasis patients induces a unique state of T-cell hyporesponsiveness. *J Invest Dermatol.* (2008) 128:1182–91. doi: 10.1038/jid.2008.4
- 49. Zgraggen S, Huggenberger R, Kerl K, Detmar M. An important role of the SDF-1/CXCR4 axis in chronic skin inflammation. *PloS One.* (2014) 9:e93665. doi: 10.1371/journal.pone.0093665
- 50. Kelley SM, Ravichandran KS. Putting the brakes on phagocytosis: "don't-eatme" signaling in physiology and disease. *EMBO Rep.* (2021) 22:e52564. doi: 10.15252/embr.202152564
- 51. Lee N, Llano M, Carretero M, Ishitani A, Navarro F, López-Botet M, et al. HLA-E is a major ligand for the natural killer inhibitory receptor CD94/NKG2A. *Proc Natl Acad Sci U.S.A.* (1998) 95:5199–204. doi: 10.1073/pnas.95.9.5199
- 52. Komine M, Karakawa M, Takekoshi T, Sakurai N, Minatani Y, Mitsui H, et al. Early inflammatory changes in the "Perilesional skin" of psoriatic plaques: is there interaction between dendritic cells and keratinocytes? *J Invest Dermatol.* (2007) 127:1915–22. doi: 10.1038/sj.jid.5700799
- 53. Cheuk S, Wikén M, Blomqvist L, Nylén S, Talme T, Ståhle M, et al. Epidermal th22 and tc17 cells form a localized disease memory in clinically healed psoriasis. *J Immunol.* (2014) 192:3111–20. doi: 10.4049/jimmunol.1302313
- 54. Keijsers RRMC, van der Velden HMJ, van Erp PEJ, de Boer-van Huizen RT, Joosten I, Koenen HJPM, et al. Balance of Treg vs. T-helper cells in the transition from symptomless to lesional psoriatic skin. . *Br J Dermatol.* (2013) 168:1294–302. doi: 10.1111/bjd.12236
- 55. Koguchi-Yoshioka H, Hoffer E, Cheuk S, Matsumura Y, Vo S, Kjellman P, et al. Skin T cells maintain their diversity and functionality in the elderly. *Commun Biol.* (2021) 4:13. doi: 10.1038/s42003-020-01551-7
- 56. Daniels J, Doukas PG, Escala MEM, Ringbloom KG, Shih DJH, Yang J, et al. Cellular origins and genetic landscape of cutaneous gamma delta T cell lymphomas. *Nat Commun.* (2020) 11:1806. doi: 10.1038/s41467-020-15572-7
- 57. McVay LD, Carding SR. Extrathymic origin of human gamma delta T cells during fetal development. J Immunol. (1996) 157:2873–82. doi: 10.4049/jimmunol. 157.7.2873
- 58. Aterido A, López-Lasanta M, Blanco F, Juan-Mas A, García-Vivar ML, Erra A, et al. Seven-chain adaptive immune receptor repertoire analysis in rheumatoid arthritis reveals novel features associated with disease and clinically relevant phenotypes. *Genome Biol.* (2024) 25:68. doi: 10.1186/s13059-024-03210-0
- 59. Sant S, Jenkins MR, Dash P, Watson KA, Wang Z, Pizzolla A, et al. Human $\gamma\delta$ T-cell receptor repertoire is shaped by influenza viruses, age and tissue compartmentalisation. *Clin Transl Immunol.* (2019) 8:e1079. doi: 10.1002/cti2.1079
- 60. Cheng C, Wang B, Gao L, Liu J, Chen X, Huang H, et al. Next generation sequencing reveals changes of the $\gamma\delta$ T cell receptor repertoires in patients with pulmonary tuberculosis. *Sci Rep.* (2018) 8:3956. doi: 10.1038/s41598-018-22061-x

61. Vermijlen D, Brouwer M, Donner C, Liesnard C, Tackoen M, Van Rysselberge M, et al. Human cytomegalovirus elicits fetal $\gamma\delta$ T cell responses in *utero. J Exp Med.* (2010) 207:807–21. doi: 10.1084/jem.20090348

- 62. Alejenef A, Pachnio A, Halawi M, Christmas SE, Moss PAH, Khan N. Cytomegalovirus drives $V\delta 2$ neg $\gamma\delta$ T cell inflation in many healthy virus carriers with increasing age. *Clin Exp Immunol.* (2014) 176:418–28. doi: 10.1111/cei.12297
- 63. Knight A, Madrigal AJ, Grace S, Sivakumaran J, Kottaridis P, Mackinnon S, et al. The role of V82-negative $\gamma\delta$ T cells during cytomegalovirus reactivation in recipients of allogeneic stem cell transplantation. *Blood.* (2010) 116:2164–72. doi: 10.1182/blood-2010-01-255166
- 64. Halary F, Pitard V, Dlubek D, Krzysiek R, de la Salle H, Merville P, et al. Shared reactivity of V δ 2neg $\gamma\delta$ T cells against cytomegalovirus-infected cells and tumor intestinal epithelial cells. *J Exp Med.* (2005) 201:1567–78. doi: 10.1084/jem.20041851
- 65. Ding Y, Ma F, Wang Z, Li B. Characteristics of the V δ 2 CDR3 sequence of peripheral $\gamma\delta$ T cells in patients with pulmonary tuberculosis and identification of a new tuberculosis-related antigen peptide. Clin Vaccine Immunol. (2015) 22:761–8. doi: 10.1128/CVI.00612-14
- 66. Gil A, Yassai MB, Naumov YN, Selin LK. Narrowing of human influenza A virus-specific T cell receptor α and β Repertoires with increasing age. *J Virol.* (2015) 89:4102–16. doi: 10.1128/JVI.03020-14
- 67. Nguyen THO, Sant S, Bird NL, Grant EJ, Clemens EB, Koutsakos M, et al. Perturbed CD8+ T cell immunity across universal influenza epitopes in the elderly. *J Leukoc Biol.* (2018) 103:321–39. doi: 10.1189/jlb.5MA0517-207R

- 68. Naumov YN, Naumova EN, Yassai MB, Kota K, Welsh RM, Selin LK. Multiple glycines in tcr α-chains determine clonally diverse nature of human T cell memory to influenza A virus. *J Immunol.* (2008) 181:7407–19. doi: 10.4049/jimmunol.181.10.7407
- 69. Vyborova A, Janssen A, Gatti L, Karaiskaki F, Yonika A, van Dooremalen S, et al. $\gamma9\delta2$ T-cell expansion and phenotypic profile are reflected in the CDR3 δ Repertoire of healthy adults. *Front Immunol.* (2022) 13:915366. doi: 10.3389/fimmu.2022.915366
- 70. Odumade OA, Weinreich MA, Jameson SC, Hogquist KA. KLF2 regulates trafficking and homeostasis of $\gamma\delta$ T cells. *J Immunol (Baltimore Md : 1950).* (2010) 184:6060. doi: 10.4049/jimmunol.1000511
- 71. García-Cuesta EM, Santiago CA, Vallejo-Díaz J, Juarranz Y, Rodríguez-Frade JM, Mellado M. The role of the CXCL12/CXCR4/ACKR3 axis in autoimmune diseases. *Front Endocrinol (Lausanne)*. (2019) 10:585. doi: 10.3389/fendo.2019.00585
- 72. Liu Y, Wang H, Cook C, Taylor MA, North JP, Hailer A, et al. Defining patient-level molecular heterogeneity in psoriasis vulgaris based on single-cell transcriptomics. *Front Immunol.* (2022) 13:842651. doi: 10.3389/fimmu.2022.842651
- 73. Zhang S. Deep analysis of skin molecular heterogeneities and their significance on the precise treatment of patients with psoriasis. Front Immunol. (2024) 15:1326502. doi: $10.3389/\mathrm{fimmu.}2024.1326502$
- 74. Ainali C, Valeyev N, Perera G, Williams A, Gudjonsson JE, Ouzounis CA, et al. Transcriptome classification reveals molecular subtypes in psoriasis. *BMC Genomics*. (2012) 13:472. doi: 10.1186/1471-2164-13-472
- 75. Guo J, Chowdhury RR, Mallajosyula V, Xie J, Dubey M, Liu Y, et al. $\gamma\delta$ T cell antigen receptor polyspecificity enables T cell responses to a broad range of immune challenges. *Proc Natl Acad Sci.* (2024) 121:e2315592121. doi: 10.1073/pnas.2315592121